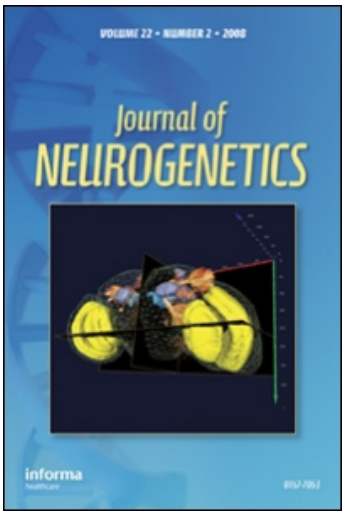

Journal of Neurogenetics
Publication details, including instructions for authors and subscription information:
http://www.informaworld.com/smpp/title~content=t713644816

The Irre Cell Recognition Module (IRM) Proteins

Karl-Friedrich Fischbach [a]; Gerit Arne Linneweber [a]; Till Felix Malte Andlauer [a]; Alexander Hertenstein [a]; Bernhard Bonengel [a]; Kokil Chaudhary [a]
[a] Department of Neurobiology, Faculty of Biology, Albert-Ludwigs-University Freiburg, Germany

First Published on: 08 January 2009

To cite this Article Fischbach, Karl-Friedrich, Linneweber, Gerit Arne, Felix Malte Andlauer, Till, Hertenstein, Alexander, Bonengel, Bernhard and Chaudhary, Kokil(2009)'The Irre Cell Recognition Module (IRM) Proteins',Journal of Neurogenetics,
To link to this Article: DOI: 10.1080/01677060802471668
URL: http://dx.doi.org/10.1080/01677060802471668

J. Neurogenetics, 2009: 1–20, iFirst article

ISSN: 0167-7063 print/1563-5260 online
DOI: 10.1080/01677060802471668

informa
healthcare

The Irre Cell Recognition Module (IRM) Proteins

Karl-Friedrich Fischbach, Gerit Arne Linneweber, Till Felix Malte Andlauer, Alexander Hertenstein, Bernhard Bonengel and Kokil Chaudhary
Department of Neurobiology, Faculty of Biology, Albert-Ludwigs-University Freiburg, Germany

Abstract: One of the most challenging problems in developmental neurosciences is to understand the establishment and maintenance of specific membrane contacts between axonal, dendritic, and glial processes in the neuropils, which eventually secure neuronal connectivity. However, underlying cell recognition events are pivotal in other tissues as well. This brief review focuses on the pleiotropic functions of a small, evolutionarily conserved group of proteins of the immunoglobulin superfamily involved in cell recognition. In *Drosophila*, this protein family comprises Irregular chiasm C/Roughest (IrreC/Rst), Kin of irre (Kirre), and their interacting protein partners, Sticks and stones (SNS) and Hibris (Hbs). For simplicity, we propose to name this ensemble of proteins the irre cell recognition module (IRM) after the first identified member of this family. Here, we summarize evidence that the IRM proteins function together in various cellular interactions, including myoblast fusion, cell sorting, axonal pathfinding, and target recognition in the optic neuropils of *Drosophila*. Understanding IRM protein function will help to unravel the epigenetic rules by which the intricate neurite networks in sensory neuropils are formed.

Keywords: myoblast fusion, cell sorting, adherence junction, planar cell polarity, target recognition, optic lobe

INTRODUCTION

While an understanding of the molecular mechanisms of wiring a brain is fundamental to developmental neurosciences, it is to be expected that mechanisms of cell recognition, membrane sorting, and the establishment of specialized cell contacts are found in other tissues as well. In some instances, these tissues present themselves as simpler systems for the analysis and functional understanding of the underlying molecular machinery. Here, we describe an ongoing quest to understand how different cell types in the fly's optic lobe establish their connections, one that turned out to benefit from experimental detours to other tissues.

The Heisenberg-Böhl method (Heisenberg & Boehl, 1979) of serially sectioning multiple paraffin-embedded fly heads simultaneously allowed the screening for mutations, causing structural brain defects in adult flies. The initial screens were restricted to the X-chromosome and used ethane methyl sulfonide (EMS) mutagenesis. The outcome of these screens resulted, among others, in the identification of the genes, *small optic lobes* (Fischbach & Heisenberg, 1981; Delaney et al., 1991) and *disco* (Steller et al., 1987; Dushay et al., 1989), and in the discovery of structural mutants of the mushroom bodies (MBs) (Heisenberg et al., 1985). A detailed description 2of the brain structure of *Drosophila* (Fischbach & Dittrich, 1989; Hanesch et al., 1989; Stocker et al., 1990), initiated in Martin Heisenberg's laboratory, encouraged us to perform a screen for *P*-element as well as X-ray–induced mutations that cause pathfinding defects in the adult brain. Among other mutants, we identified two alleles of an X-chromosomal complementation group, which we initially called *irregular chiasm C (irreC)*. Significantly, the *P*-element–induced allele, *UB883*, and the X-ray–induced allele, *1R34*, were found to cause misrouting of fibers in the first and second optic chiasms at high, allele-specific frequencies (Boschert et al., 1990). Genetic mosaic analysis showed that these mutant phenotypes do not depend on the eye genotype, and the defects in the chiasms were statistically independent of each other. It was concluded that the gene is functioning in at least two neural cell populations, one participating in the formation of the first chiasm, the other in the formation of the second optic chiasm. Ramos et al. (1993) found that *roughest* (*rst)* and *irreC* alleles map to the same gene, which is expressed in the eye and in cell populations of the optic lobe. Hence, the gene is called *irreC*/*rst*.

Received 13 August 2008; Revised 25 August 2008; Accepted 10 September 2008.
Address correspondence to Karl-Friedrich Fischbach, Institute for Biology III, Faculty of Biology, Schänzlestr. 1, D-79104 Freiburg i. Brsg., Germany. E-mail: kff@uni-freiburg.de

The molecular analysis of the *irreC/rst* gene revealed that it codes for a single-pass transmembrane protein of the immunoglobulin (Ig) superfamily with five extracellular Ig-domains, where the first two Ig-domains of IrreC/Rst more closely resemble the V-type and the inner three domains more the C-type of Ig-domains (Ramos et al., 1993). *Drosophila irreC/rst* was thus the first gene found to code for a member of the Ig superfamily following the initial description of a mutant axonal pathfinding defect. Since then, a *Drosophila* paralog of IrreC/Rst has been described, kin of irre (Kirre, also called Dumbfounded; Ruiz-Gomez et al., 2000; Strünkelnberg et al., 2001). In addition, the heterophilic binding partners of both paralogs, sticks and stones (SNS; Bour et al., 2000; Galletta et al., 2004) and hibris (Hbs; Artero et al., 2001, Dworak et al., 2001), have been found in *Drosophila*, and orthologs of these proteins have been identified in other species, ranging from *Caenorhabditis elegans* to humans (see Table 1, Figure 1).

Table 1. Irre cell recogniton module proteins (IRM Proteins)

	Kirre/NEPH-like subfamily	*SNS/nephrin-like subfamily*
		
D. melanogaster		
	IrreC/Roughest	*Hibris (Hbs)*
Expressed in: (1–5)	Fusion-competent myoblasts Muscle founder cells Apodemes Interommatidial precursors Nervous system Cells of the anterior wing margin	Fusion-competent myoblasts (4) Primary pigment cells (3, 5) Many interneurons (3) Cells of the anterior wing margin
Interactions:	Hibris, SNS, X11Lα (3, 5, 6)	SNS, IrreC/Rst (3, 5)
Functions:	Axonal pathfinding, myoblast fusion, cell sorting in imaginal discs, neural target selection (10)	Myoblast fusion, cell sorting in imaginal discs
	Kirre/Dumbfounded	*Sticks and Stones (SNS)*
Expressed in:	Muscle founder cells (1, 8) Interommatidial precursors (3) Nervous system (3) Anterior wing margin (3)	Fusion-competent myoblasts (9) Primary pigment cells (3) Bristle cells in the eye (3) Nervous system (3) SOPs of the anterior wing margin (3)
Interactions:	SNS, X11Lα, Rols7 (6, 10, 11)	Kirre, Crk > D-WIP/Sltr > Wsp > Arp2/3 (12, 13)
Functions:	Myoblast fusion (1, 8)	Myoblast fusion (9)
C. elegans		
	SYG-1	*SYG-2*
Expressed in:	HSNL neuron	Vulval epithelial cells
Interactions:	extracell.: SYG-2 intracell.: SYD-1 > SYD-2 > CASK	extracell.: SYG-1
Functions:	SYG-1 and SYG-2 mediate recognition between the HSNL neuron and guidepost cells. SYG-1 directs the localization of the presynaptic machinery to contact sites (14–16)	
Mammals		
	mKirrel, NEPH1, NEPH2, NEPH3	*Nephrin*
Expressed in: (17–20)	Bone marrow stromal cells Podocytes Central nervous system	Podocytes
Interactions: (19–22)	Nephrin, metalloproteinases, CASK, podocin, ZO-1, Par3 > aPKC > Par6 > CDC42	Podocin (23), NEPH1, NEPH2 (24), Fyn (25) PI3K (27), CD2AP > WASp > CAPZ > Arp2/3 (26)
Functions: (17, 25)	Support of hemat. stem cells Podocyte development	Podocyte development (18)

Citations: (1) Strünkelnberg et al. (2001); (2) Reiter et al. (1996); (3) in preparation; (4) Artero et al. (2001); (5) Bao & Cagan, (2005); (6) Vishnu et al. (2006); (7) Bazigou et al. (2007); (8) Ruiz-Gomez et al. (2000); (9) Bour et al. (2000); (10) Galletta et al. (2004); (11) Patel et. al. (2006); (12) Shen & Bargmann (2003); (13) Shen et al. (2004); (14) Kreisköther et al. (2006); (15) Kim et al. (2007); (16) Massarwa et al. (2007); (17) Ueno et al. (2003); (18) Kestilä et al. (1998); (19) Sellin et al. (2002); (20) Gerke et al. (2006); (21,23) Huber et al. (2003b,b, c); (22) Liu et al. (2003); (24) Gerke et al. (2005); (25) Verma et al. (2003); (26) Huber & Benzing (2005); (27) Huber et al. (2003a).

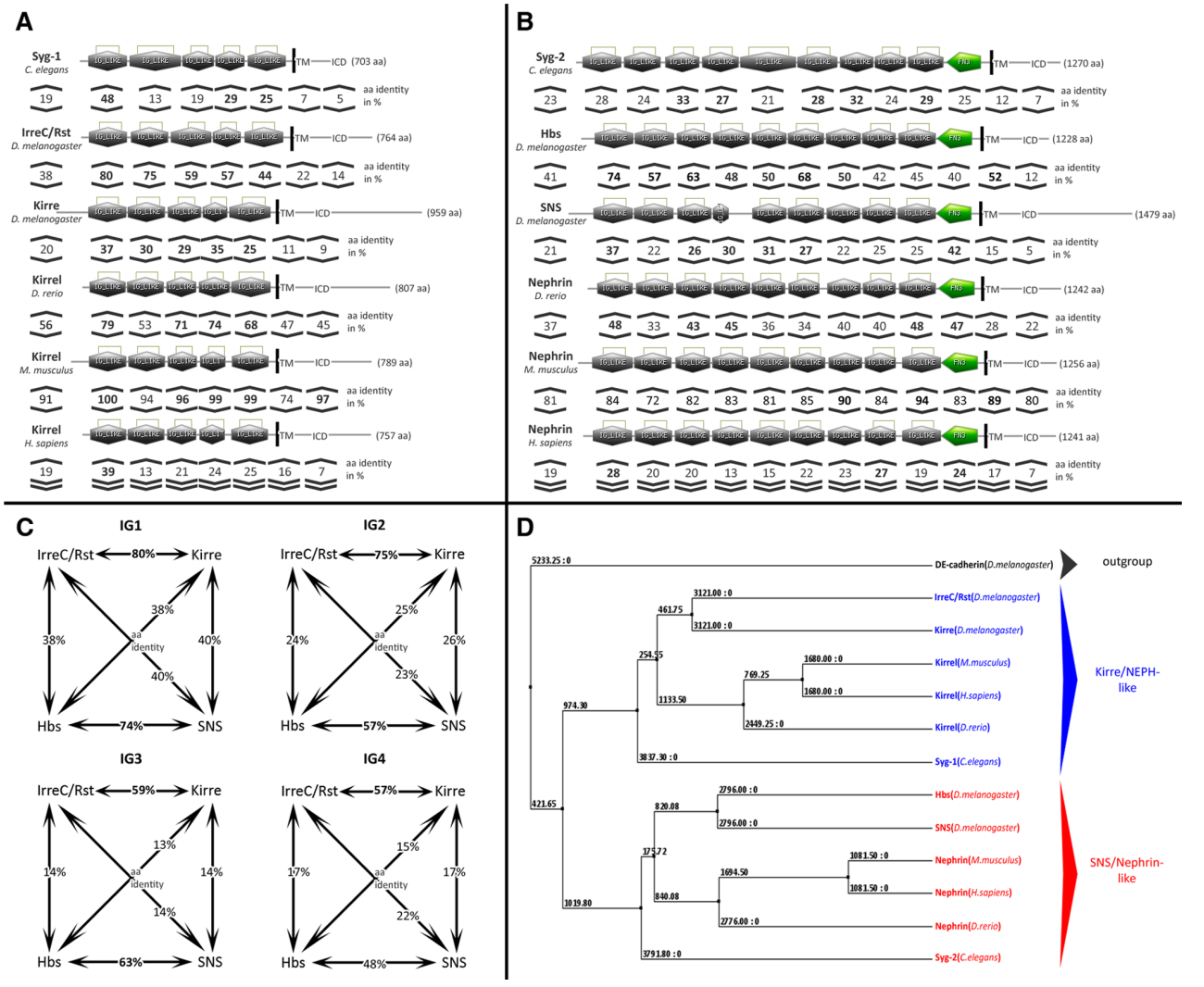

Figure 1. Sequence analysis of the irre cell recognition module (IRM) proteins. Protein domains in the figures were identified by using the Prosite domain prediction software (Bairoch, 1991) to ensure that the same algorithm was used for all proteins. Transmembrane (TM) domains were defined by using TMpred (Hofmann & Stoffel, 1993). Sequences were aligned by using clustalW (Thompson et al., 1994), and for the domains defined by Strünkelnberg et al. (2001), an alignment was compiled and the amino acid (aa) identity was calculated between the sequences. In cases where the identity for a single domain was 5% higher than the identity of the whole protein, numbers are written in bold. In addition, the identities for the intracellular domains (ICDs) are shown. (**A**) Detailed analysis of aa identity of the domains of the Kirre/NEPH-like proteins, SYG-1, IrreC/Rst, Kirre, and Kirrel, from three different species. The most N-terminal Ig-domain is particularly well conserved between all species pairs. The other four Ig-domains are less conserved, and the lowest conservation is found between the TM domains and the ICDs. (**B**) Detailed analysis of an identity of the domains of the SNS/Nephrin-like proteins, SYG-2, Hbs, SNS, and Nephrin, from three different species. When domains could not be identified with the Prosite algorithm, the annotated domains were used (marked with an asterisk). The high conservation of Nephrin proteins between mouse and humans is particular striking. The human Nephrin has still a 19% aa identity, compared to SYG-2. All proteins show a higher conservation of the extracellular domains relative to the other parts of the polypeptide, while the TM domain is only strongly conserved between Hbs and SNS and between mouse and human Nephrin. The intracellular domain is never well conserved. (**C**) Analysis of the conservation between the *Drosophila melanogaster* proteins, IrreC/Rst, Kirre, SNS, and Hbs. A similar analysis was performed as in **A** and **B**, with the difference that only these four proteins were aligned. (**D**) Average distance tree of an alignment of all Kirre/NEPH-like and SNS/Nephrin-like proteins of **A** and **B** and—as an outgroup—DE-cadherin from *D. melanogaster*. A Blossum 62 similarity was used to define distances. The tree was constructed by using Jalview (Clamp et al., 2004), based on a clustalW2 multiple sequence alignment. As expected, the tree contains three groups of proteins: the outgroup, the kirre/NEPH-like proteins, and the SNS/Nephrin-like proteins. Numbers refer to the Blossum 62 similarity and the corresponding Bootstrap values.

THE IRRE CELL RECOGNITION MODULE PROTEINS IN *DROSOPHILA* AND OTHER SPECIES

Figure 1 illustrates the sequence comparison of these proteins from different species. The numbers indicate the amino acid (aa) sequence identity between the corresponding orthologous and paralogous proteins. The proteins fall into two subclasses. The shorter Kirre/NEPH-like proteins are aligned in Figure 1A and the SNS/nephrin-like proteins in Figure 1B. In addition to the larger number of Ig-domains, SNS/Nephrins differ from Kirre/NEPH proteins in their extracellular region by a fibronectin type III domain flanking the transmembrane domain. In SNS/nephrins as well as in kirre/NEPHs, the conservation of the aa sequence is the strongest for the outer N-terminal Ig-domain and decreases toward the transmembrane domain (Figure 1; Strünkelnberg et al., 2001). It is noteworthy that the intracellular domains of SNS/Nephrins and Kirre/NEPHs are highly variable. Interestingly, the Ig-domains of the Kirre/NEPH-like and SNS/Nephrin-like proteins closest to the N-terminal are related (Figure 1C). The well-established heterophilic interactions between Kirre/NEPH-like and SNS/Nephrin-like proteins in *C. elegans* (Shen et al., 2004), *Drosophila* (Galletta et al., 2004; Bao & Cagan, 2005), and vertebrates (Liu et al., 2003; Gerke et al., 2005) may thus have evolved from homophilic interactions of an early common ancestor.

It is worth mentioning that the vertebrate members of the two protein subfamilies were first identified in podocytes of the kidney (Kestilä et al., 1998; Sellin et al., 2002). Podocytes have several distinct cell biological features in common with neurons, for example, they possess long and short cell processes equipped with a highly organized cytoskeleton and they express a number of otherwise neuron-specific proteins (e.g., the actin-associated, spine-specific synaptopodin; Mundel et al., 1997). The slit membrane between foot processes of podocytes forms the important ultrafiltration barrier of the kidney and may represent a modified adherens junction (Rose & Post, 2001). Because of their essential function in building the slit membrane, much attention has been paid to the interactions of irre cell recognition module (IRM) proteins in the kidney. In podocytes, Nephrin signaling is facilitated by its recruitment to lipid rafts by podocin (Huber et al., 2003b). Nephrin promotes cell-cell adhesion through homophilic interactions and shows heterophilic interactions as well (Gerke et al., 2003, 2005). The emerging picture is that the Ig-domains of NEPH1 and Nephrin form promiscuous homo- and heterophilic interactions that may facilitate di- or oligomerization in *cis* and in *trans* at the glomerular slit diaphragm. It was shown by Huber et al. (2003a) that NEPH1, NEPH2, and NEPH3 bind the PSD95/Dlg/ZO-1 (PDZ) domain-containing protein, zonula occludens-1 (ZO-1), mediated by their PDZ binding motif at the carboxyl terminus. ZO-1 binding is associated with a strong increase in tyrosine phosphorylation of NEPH1 and dramatically increases the ability of NEPH1 to mediate signal transduction. Thus, the PDZ-domain protein seems to spatially organize NEPH proteins and has the ability to recruit signal-transduction components (Huber et al., 2003a). In analogy, *Drosophila* IrreC/Rst binds X11Lα/Mint1 with its PDZ-binding domain in the retina (Vishnu et al., 2006). Nephrin is intracellularly phosphorylated by Fyn tyrosin kinase—this is essential for its potential to bind phosphoinositide 3 kinase and also significantly enhances the binding of Fyn itself (Liu et al., 2005).

For simplicity, we propose to use the acronym IRM for the ensemble of the Kirre/NEPH- and SNS/Nephrin subfamilies. This gives reference to the first member identified and conveys an idea about their proposed cooperative function in different tissues. The following sections will summarize our current knowledge of IRM proteins in *Drosophila*.

IRM PROTEINS MEDIATE MYOBLAST FUSION

There are four known IRM members in *Drosophila*, the short IrreC/Rst and kirre, and their heterophilic interaction partners, the longer Hbs and SNS (Table 1, Figure 1). These proteins form a functional unit, which is best understood in myoblast fusion (Figure 2). Muscles in *Drosophila* develop from a single myotube, which originates from the fusion of two kinds of cell types, a founder cell that gives the muscle its identity, and many fusion-competent myoblasts (FCMs) that deliver nuclei and cytoplasm. Fusion is never observed between cells of either type alone. This asymmetric fusion process thus requires the attraction and recognition of FCMs to muscle founder cells and the growing myotubes (Doberstein et al., 1997). Among the IRM genes, the *sns* gene, which is specifically expressed in FCMs, is essential for this process. *sns* mutations block the fusion of the competent myoblasts with the growing myotubes (Bour et al., 2000). Hbs, like SNS, is only present in FCMs and plays a regulatory role (Artero et al., 2001).

IrreC/Rst and Kirre act in a redundant fashion during myoblast fusion. The deletion of both genes leads to a lethal muscle phenotype (Strünkelnberg et al., 2001). Kirre is exclusively located on founder cells and growing myotubes (Ruiz-Gomez et al., 2000), whereas IrreC/Rst is present on FCMs and on founder cells (Strünkelnberg et al., 2001). Either protein has the capacity to attract FCMs, and at least one of them is required in order for myoblast fusion to occur (Ruiz-Gomez et al., 2000; Strünkelnberg et al., 2001). It is being discussed whether

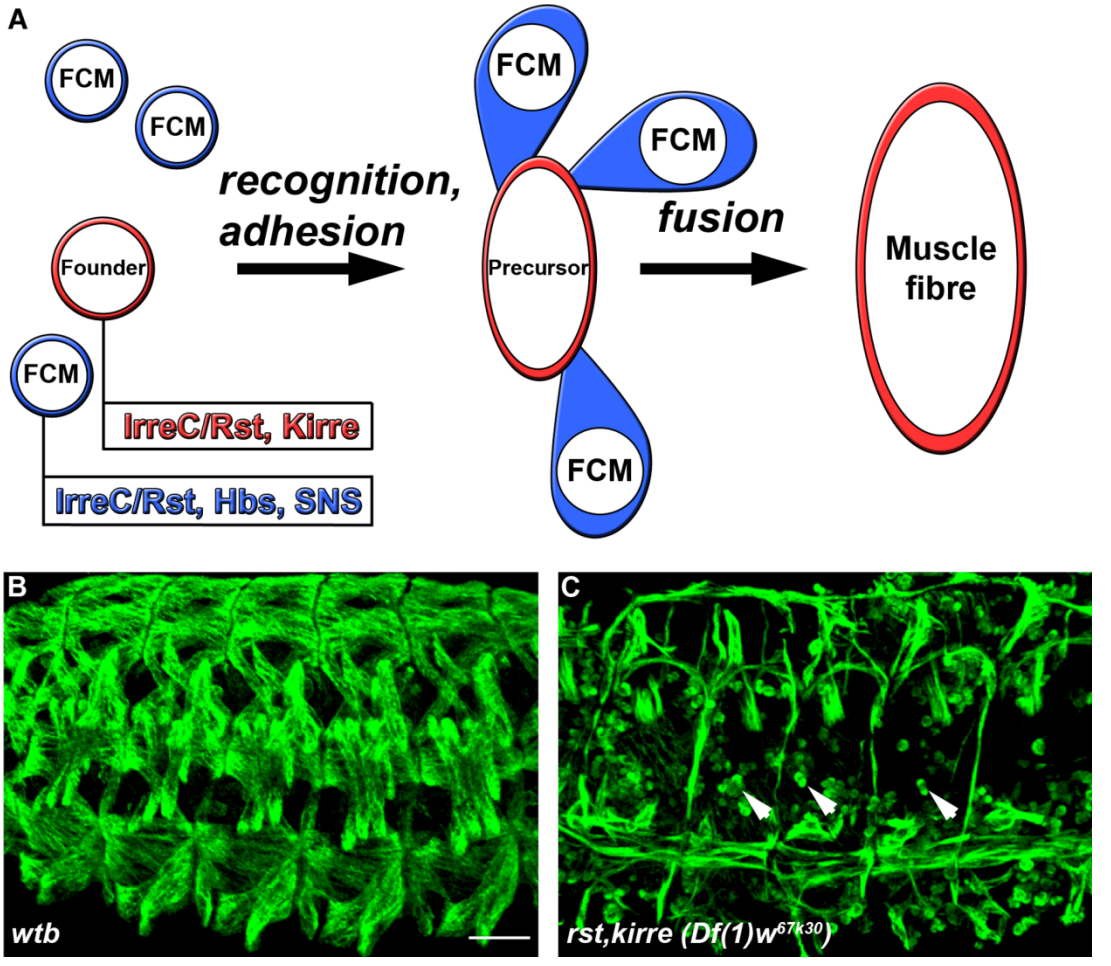

Figure 2. Irre cell recognition module (IRM) proteins mediate myoblast fusion. Differential expression of the IRM proteins in fusion-competent myoblasts and in founder cells is required for recognition between these cell types. (**A**) Schematic view of the process. (**B**) Wild-type muscle pattern visualized by a ß-3-tubulin antibody. (**C**) Mutant phenotype when both Kirre and IrreC/Rst are missing. The small, round fusion-competent myoblasts have not fused with the muscle fibers and are still visible at stage 16 (arrow heads). Scale bar, 20 μm.

the extracellular domains of Kirre or IrreC/Rst can be cleaved by metalloproteases, thereby forming a diffusion gradient helping FCMs to navigate (Chen & Olson, 2004; Gerke et al., 2005; Menon et al., 2005). An alternative mechanism for the establishment of an initial mechanical contact between FCMs and founder cells may be an exploratory behavior of FCMs via a single, distinct filopodial process that they use to ''sense'' their environment (Doberstein et al., 1997; Ruiz-Gomez et al., 2000). The contact that is formed between FCMs and founder cells and myotubes prior to fusion is highly specialized and has a ring-like appearance when visualized with antibodies against SNS, Kirre, or Rols7—a multidomain protein that interacts with both Kirre and SNS. This structure has been called ''FuRMAS'' (fusion-restricted myogenetic-adhesive structure), and it surrounds an F-actin core in both the myotube and the FCMs (Kesper et al., 2007). The IRM proteins are not only crucial for the fusion process in the way that they establish the first contact between the fusing cells by virtue of the heterophilic binding of their extracellular domains, but they are also instrumental in initiating the next steps via signaling. Galletta et al. (2004) showed that the cytoplasmic and transmembrane domains of SNS are essential for the fusion of embryonic myoblasts, while the extracellular domain of SNS is sufficient to mediate heterophilic binding when anchored to the membrane via GPI in S2 cells.

Prior to fusion SNS is involved in signaling, causing Wsp-dependent F-actin polymerization (Wsp is the *Drosophila* homolog of the WASp family of microfilament nucleation-promoting factors; Kim et al., 2007). The link between SNS and Wsp is mediated by the Wsp interacting protein (D-WIP/solitary) and DCrk that directly binds to SNS (Menon & Chia, 2007). Kocherlakota et al. (2008) found that during myoblast fusion,

the intracellular domain of SNS most likely acts through its multiple phosphotyrosine sites as well as through a proline-rich region. Remarkably, highly conserved consensus sites for binding postsynaptic density-95/disc large/zonula occludens-1-domain containing (PDZ) proteins and several serine phosphorylation sites of SNS appear not to be involved in myoblast fusion.

In the growing myoblast, the intracellular domain of Kirre binds to the tetratricopeptide repeats (TPRs) of the adaptor protein, antisocial/rolling pebbles (Rols; Chen & Olson, 2001; Rau et al., 2001; Kreisköther et al., 2006), which, in turn, recruits myoblast city (Mbc), the *Drosophila* homolog of DOCK180/CED-5 (Nolan et al., 1998; Pütz et al., 2005). Mbc then recruits the SH2-SH3 adaptor protein, DCrk (Pütz et al., 2005). It was, therefore, long believed that the signaling pathway involves mainly the activation of the small GTPase, Rac1. However, Balagopalan et al. (2006) showed that the interaction of Mbc with DCrk is not essential for myoblast fusion. Instead, they found that the conserved DHR1 domain of Mbc, which binds phosphatidylinositol 3,4,5-triphosphate, is required.

The myoblast fusion pathway seems to be conserved in *Drosophila* and in vertebrates. For example, it was found that the zebrafish ortholog of Kirre, Kirrel, is required for myoblast fusion in this species (Srinivas et al., 2007). The myoblast fusion process clearly shows that IRM proteins are able to initiate intracellular differentiation events upon establishing an asymmetrical cellular contact between different polarized cell types. The resulting working hypothesis is that the common denominator of IRM function in myoblast fusion, and in the development of other tissues, is the mediation of asymmetrical contacts between different cell types. Although the genes for the relevant proteins are differentially expressed, they are located on opposing cell membranes and cause their close apposition. This behavior of the proteins underlies the amazingly similar patterns of immunoreactivity in the eye and wing imaginal disc as well as in the pupal optic lobe (Figure 3).

IRM PROTEINS MEDIATE SORTING OF CELL TYPES IN THE PUPAL EYE IMAGINAL DISC

At about 16% of pupal development, after completion of ommatidial development, each presumptive facet is capped by four cone cells and surrounded by an outer ring built of two primary pigment cells (PPCs). The ommatidia are still ''swimming'' among an unidentified number of interommatidial precursor cells (IPCs). Wolff and Ready (1991) described the normal sorting of IPCs into a single row and the subsequent elimination of surplus cells via apoptosis. They also showed that the cell-sorting process is severely disturbed in rst^{CT} mutants. Ramos et al. (1993) demonstrated that the rst^{CT} mutation is a 98-base pair (bp) deletion, resulting in a mutant protein, where the C-terminal 175 aa of the wild-type intracellular domain are replaced by a new polypeptide of 63 aa due to the frame shift. Signaling, rather than adhesion, should be affected.

Subsequently, the involvement of IrreC/Rst in eye development was analyzed more closely (Reiter et al., 1996; Gorski et al., 2000; Bao & Cagan, 2005; Grzeschik & Knust, 2005). The protein is dynamically expressed in a succession of cell types during eye development, as described in detail by Reiter et al. (1996) (Figure 4). Here, we focus on the developmental stages where cell sorting occurs and on the apical cellular contacts in the eye imaginal disc. At 12% of pupal development, all membrane contacts among IPCs show equal IrreC/Rst immunoreactivity, whereas membranes of developing PPCs display a stronger staining intensity. After the PPCs have surrounded the cone-cell quartet, IrreC/Rst is seen to accumulate at the membrane contacts of IPCs to PPCs (16% pupal development). The border between these two cell types was originally straight, but now it develops an involuted contour, (i.e., PPCs seem to squeeze in between neighboring contacts of two IPCs). During 16–21% of pupal development, the IPCs reorganize into chains lying end to end and the preferential accumulation of the IrreC/Rst protein at the IPC/PPC interface is retained. Even later, at 23% of pupal development, IrreC/Rst at IPC/IPC borders is completely removed and the protein persists only at IPC/PPC borders (Reiter et al., 1996), although *in situ* hybridization experiments have shown that, at this stage, mRNA is mainly present in IPCs (Ramos et al., 1993).

Ectopic expression of IrreC/Rst in cone cells severely disturbs the sorting process of IPCs and an accumulation of IrreC/Rst at the IPC/PPC interface cannot be observed anymore. To explain this effect, Reiter et al. (1996) postulated the existence of a heterophilic ligand inside PPCs that is relocated to the cone-cell/PPC boundary. Bao and Cagan (2005) identified Hbs in PPCs and showed that its preferential adhesion to IrreC/Rst is required for cell sorting to occur. We, here, provide direct evidence that ectopic IrreC/Rst in cone cells can, indeed, relocalize Hbs inside PPCs to the cone-cell/PPC interface. The same is true for SNS, which is present in PPCs as well (Figure 5). In this experimental situation, Kirre localization is also altered, and it persists in the apical contacts of IPCs with each other (Figure 5G–5I).

The mutual influence of the IRM proteins on each other is also supported when the rst^{CT} mutant is analyzed. The intracellularly truncated rst^{CT} mutant protein is still detectable with Mab24A5.1, which is directed against an epitope of the extracellular domain (Schneider et al., 1995). In Figure 6, it is shown that the mutant protein is no longer distributed homogeneously along the PPC/IPC interface, being clustered instead. After what we have

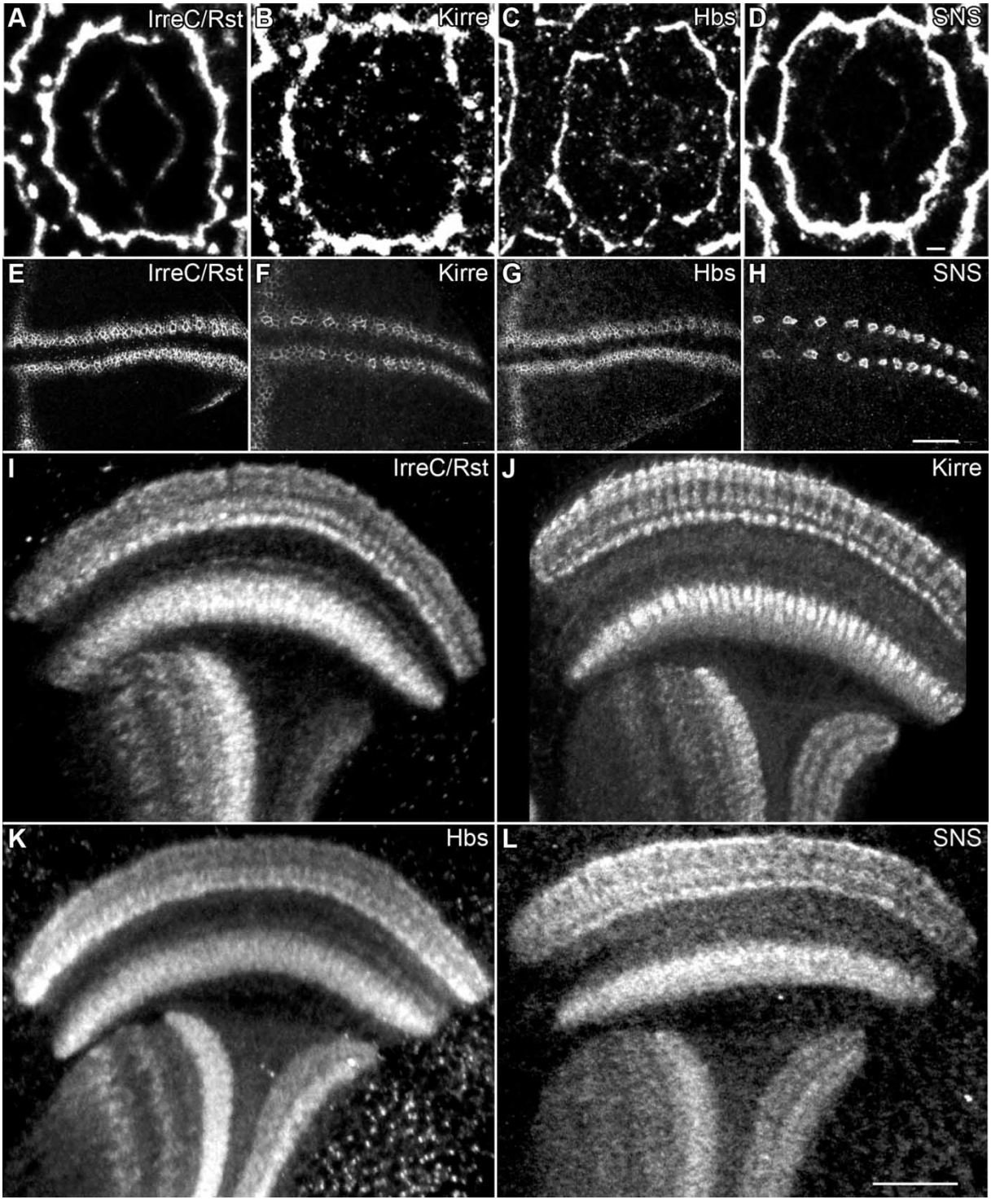

Figure 3. Irre cell recognition module (IRM) protein localization in the eye and wing imaginal discs and in the pupal optic lobe. The four IRM proteins mediate heterophilic membrane contacts between polarized cell types and are consequently expressed in close proximity. This is exemplified by their immunoreactivities in the eye at 25% pupal development (**A**–**D**; scale bar, 1 μm) and wing at L3 imaginal discs (**E**–**H**; scale bar, 20 μm) and in the optic lobe at 60% pupal development (**I**–**L**; scale bar, 50 μm). Antibodies used were anti Kirre (A126i; Kreisköther et al., 2006), anti-IrreC/Rst (Mab24A5.1; Schneider et al., 1995), anti-SNS (Kesper et al., 2007), and a newly designed polyclonal antibody against the intracellular domain of hibris (Hbs) (AS14).

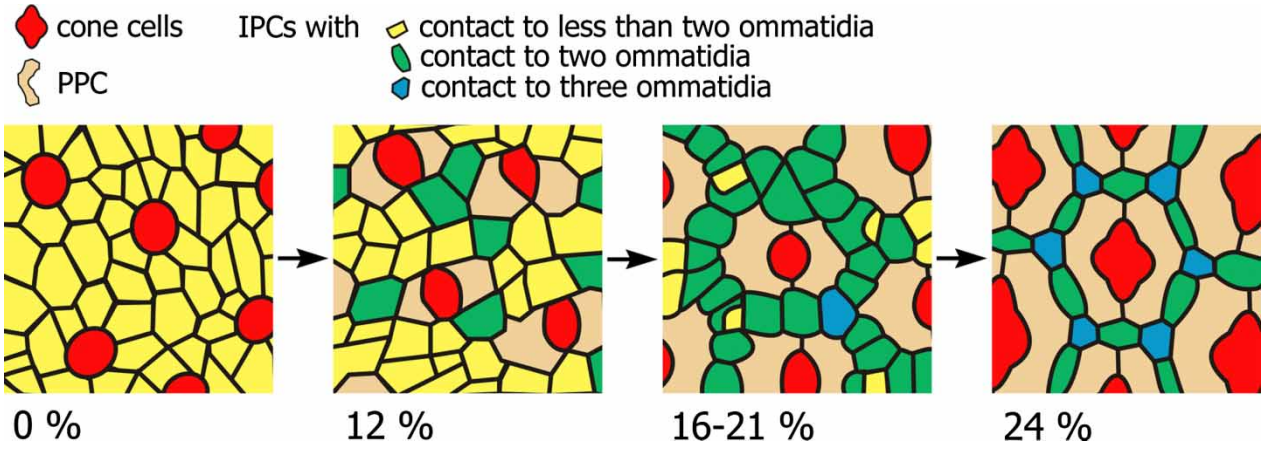

Figure 4. Formation of the cellular crystal and establishment of the planar polarity of the compound eye. First transition: Primary pigment cells (PPCs; light brown) form around the cone-cell quartet (red). Second transition: sorting of interommatidial precursors (IPCs) into a single row. Third transition: the reduction of cell numbers by programmed cell death. The IPCs are color coded according to the number of contacts they form to ommatidia (yellow for less than two contacts, green for two, and blue for three contacts). The number of green and blue cells increases during this formation of the highly ordered cellular crystal of the compound eye. The percentages given describe the progress of pupal development. Modified after Reiter et al. (1996).

learned from the overexpression studies, it is not too surprising that localization of all the other IRM proteins is altered as well. In fact, SNS and Hbs proteins cocluster at the PPC/IPC border with the rst^{CT} mutant protein, while much of the kirre protein is localized at the IPC/IPC contact sites in the mutant (Figure 6).

The normal localization of the IrreC/Rst protein in the eye imaginal disc is dependent on the proper functioning of the Delta/Notch signaling pathway and mutations in either gene can affect IrreC/Rst protein localization (Reiter et al., 1996; Gorski et al., 2000). In males carrying hemizygously the *Notch* allele, *facet strawberry* (fa^{swb}), only some cells in eye imaginal discs display the typical shape of PPCs. Sorting of IPC occurs only in the neighborhood of such differentiated PPCs, and only in such regions do the IPC/IPC contacts become depleted of IrreC/Rst and does the protein accumulate at the borders to the PPCs as it does in wild type. Such differentiated PPCs always express SNS and Hbs at the cell membranes contacting IPCs (Figure 7A and 7B). In eye imaginal discs, mutant for the *facet glossy* (fa^{gl}) *Notch* allele, no differentiated PPCs can be seen, sorting of IPCs fails completely, and IrreC/Rst is present at the IPC/IPC interface (Reiter et al., 1996; Figure 7D–7F). In this mutant eye imaginal disc, SNS expression is only retained in the bristle precursors (Figure 7D), while Hbs is visible along the cone-cell quartet/PPC interface, where it colocalizes with IrreC/Rst (Figure 7E), which is known to be expressed in cone cells (Reiter et al., 1996). Kirre is strongly localized at IPC/IPC contacts in both *facet* mutants at 25% of pupal development. In fa^{gl}, it colocalizes completely with IrreC/Rst (Figure 7F).

Cell sorting in the eye imaginal disc and the proper localization of IrreC/Rst require a continuous belt of the homophilic cell-adhesion protein, DE-cadherin, at the apical end of the IPCs (Grzeschik & Knust, 2005). Based on what we have learned, we hypothesize that this belt will also be required to directly or indirectly stabilize the other IRM proteins. The IRM proteins add asymmetry (i.e., planar cell polarity) to the symmetrical DE-cadherin interaction of the cells at the apical adherence junctions in the eye imaginal disc.

IRM PROTEINS PATTERN THE REGULAR ARRAY OF SENSORY BRISTLES

IRM gene expression is not restricted to the imaginal disc of the eye. Reddy et al. (1999) demonstrated the involvement of IrreC/Rst in olfactory sense organ spacing on the third segment of the antenna, where it influences the positioning, rather than the number, of founder cells on the antennal disc ectoderm. The third antennal segment is divided into three regions, one of which is exclusively occupied by trichoid sensilla (TS), the second one by basiconic sensilla (BS), and the third one is a region of overlap. In wild type, BS are separated by intervening hairs. This is not the case in the rst^{CT} mutant and in transformant flies, in which *irreC*/*rst* has been uniformly misexpressed (Reddy et al., 1999). In wild-type larvae, IrreC/Rst is found in late third instar antennal discs in the semielliptical domains I–IV. Expression is, at first, uniform on apical profiles of cells. With progressing differentiation, homogeneous expression decreases and immunoreactivity concentrates around the apical lateral

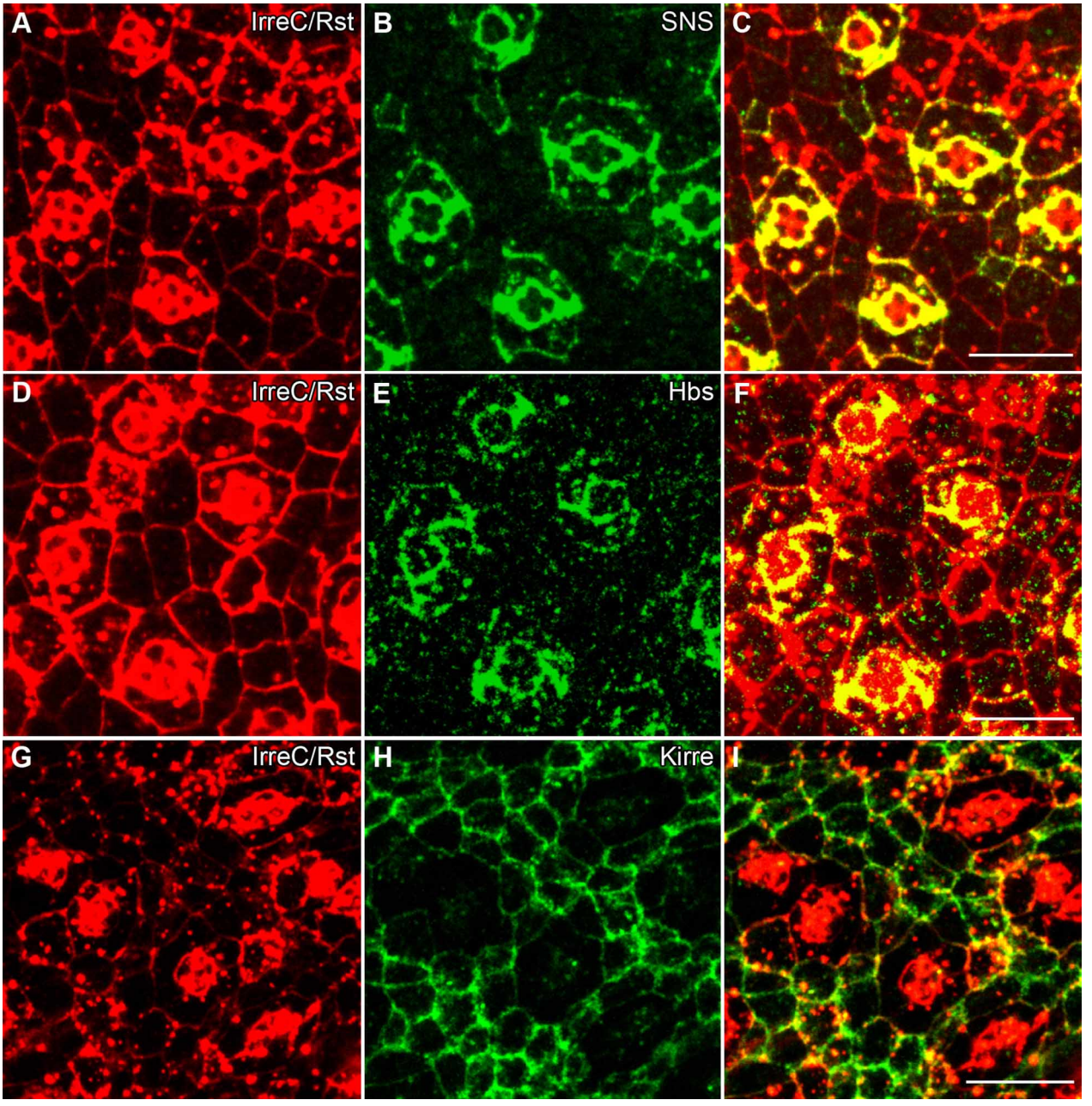

Figure 5. Ectopic expression of irregular chiasm C/roughest (IrreC/Rst) in cone cells leads to an altered localization of Hbs, SNS, and Kirre. Each row shows a different eye imaginal disc of the sev-GAL4/$^{+}$; UAS-IrreC/Rst/$^{+}$ genotype at 25% pupal development. These eye imaginal discs were all stained with anti-IrreC/Rst (Mab24A5.1; red) and individually (green), either by anti-SNS (Bour et al., 2000), anti-Hbs (Artero et al., 2001), or antikirre (A126i). When compared to the wild-type protein localization in Figure 3A–D, SNS and Hbs immunoreactivities inside primary pigment cells (PPCs) are no longer strongest at the PPC/interommatidial precursor cell (IPC) borders, but accumulate at PPC/PPC and PPC/cone-cell borders. Kirre is now seen at IPC/IPC contact sites. Scale bar, 10 μm.

cell contacts of the sense organ founder cells. While the surrounding cells display weak, grainy IrreC/Rst immunoreactivity, the cell in the center shows no cytoplasmic localization. Although, the other members of the IRM were not yet identified in 1999, these data of Reddy et al. (1999) strongly suggest that IRM function is not confined to eye development, but may be generalized to other imaginal discs as well. In fact, the availability of antibodies against all four IRM members has confirmed their colocalization in the semielliptical neurogenic domains of the antennal disc (data not shown). Further, we found all four IRM proteins to be expressed in the neurogenic region at the presumptive anterior wing margin, where sensory bristles develop (Figure 3E–3H).

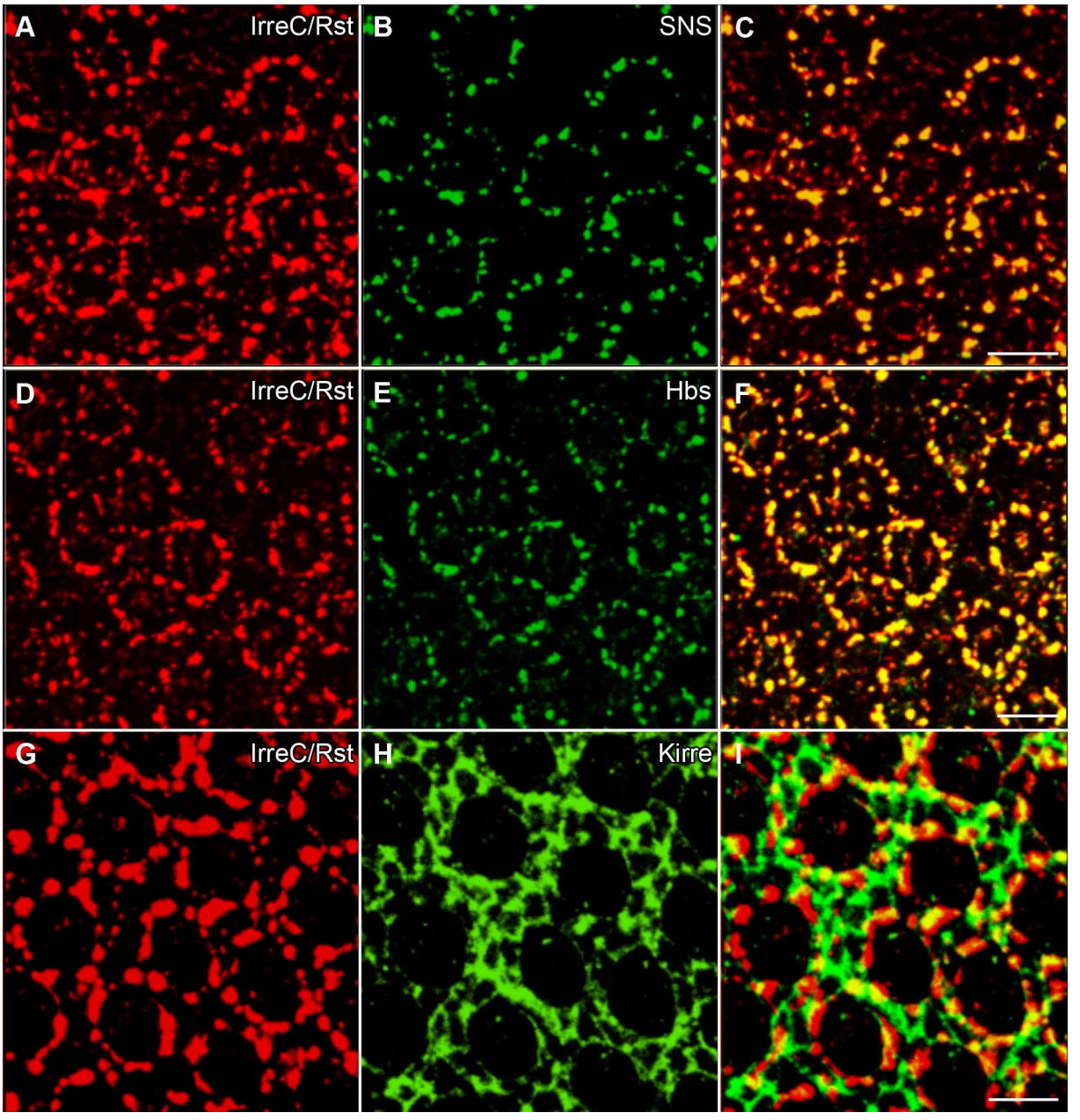

Figure 6. A partial deletion of the intracellular domain of irregular chiasm C/roughest (IrreC/Rst) in rst^{CT} mutants leads to an altered localization of all irre cell recognition module (IRM) proteins. Each row shows a different eye imaginal disc of rst^{CT}/Y genotype at 25% pupal development. These eye imaginal discs were all stained with Mab24A5.1 (red) and individually (green), either by anti–sticks and stones (SNS) (Bour et al., 2000), anti-hibris (Hbs) (Artero et al., 2001), or antikirre (A126i). When compared to the wild-type protein localization in Figure 3, immunoreactivities of SNS (**B**) and Hbs (**E**) cluster together with the truncated IrreC/Rst protein (**C**, **F**) at the primary pigment cell/interommatidial precursor cell (PPC/IPC) borders, while kirre (**H**, **I**) is now mainly seen at IPC/IPC contacts. No cell sorting has occurred. Scale bar, 10 μm.

Sensory organ precursors (SOPs) of chemosensory recurved bristles of the anterior wing margin are normally separated by several epidermal cells. In the adult fly, the recurved bristles are spaced, on average, 4.4 cell diameters on the dorsal and 3.8 cell diameters on the ventral side of the triple row of *wtb* (Hartenstein & Posakony, 1989). Here, we provide evidence that the proteins of the IRM are required for the regular-shaped array of bristles at the anterior wing margin (Linneweber et al., in preparation). The expression of all four proteins in stage L3 is strongest in the neurogenic region of the presumptive anterior wing margin and in the presumptive wing veins (Figure 3E–3H). Three IRM proteins, IrreC/Rst, kirre and Hbs, colocalize. All three can be found at

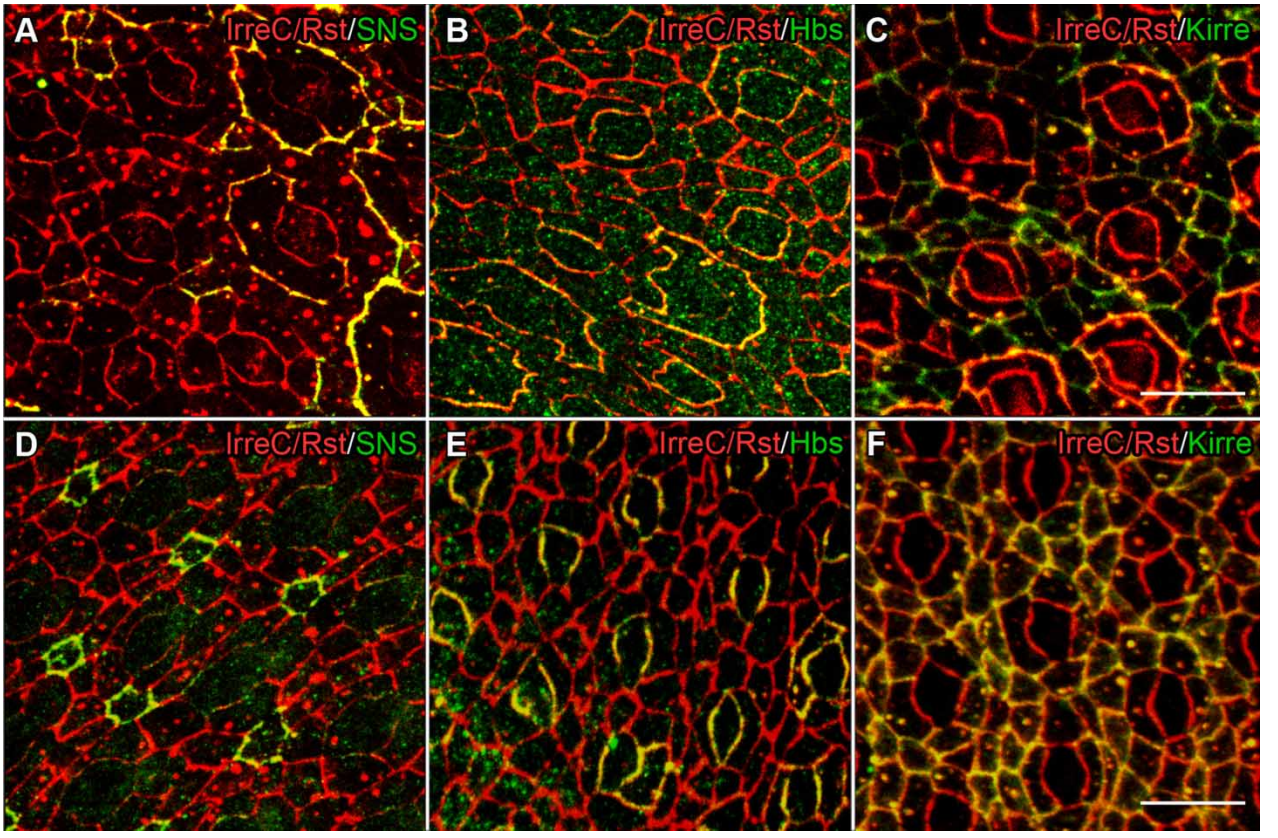

Figure 7. Notch mutations strongly alter the localization of irre cell recognition module (IRM) proteins. The upper row (**A**–**C**) depicts three eye imaginal discs of fa^{swb}/Y pupae at 25% pupal development, the lower row (**D**–**F**) shows three eye imaginal discs of fa^{gl}/Y pupae at about the same developmental time. All six imaginal discs have been incubated with anti–irregular chiasm C/roughest (IrreC/Rst) (red). Sticks and stones (SNS) in the first, hibris (Hbs) in the second, and kirre in the third column are shown in green. In fa^{swb}/Y, only a few primary pigment cells (PPCs) differentiate. At the borders of such PPCs to interommatidial precursor cells (IPCs) SNS (**A**), Hbs (**B**), and kirre (**C**), immunoreactivity can be observed to colocalize with IrreC/Rst (**A**–**C**). In the neighborhood of differentiated PPCs, IrreC/Rst is depleted from IPC/IPC interfaces (**A**). In fa^{gl}/Y pupae, SNS is only visible around the bristle complex (**D**), while Hbs inside semidifferentiated PPCs is located at the PPC/cone-cell border (**E**). Cone cells are known to contain IrreC/Rst (Reiter et al., 1996) that heterophilically binds to Hbs (Bao & Cagan, 2005). Kirre is located in both *facet* mutants at IPC/IPC contacts (**C**, **F**). Scale bar, 10 μm.

the borders of all cells in the neurogenic region. They are enriched around the SOPs that give rise to the recurved bristles. The distribution of these proteins differs only in the width of the immunoreactive stripes and in the strength of the staining of the presumptive wing veins. IrreC/Rst expression shows the thinnest band of the three and displays the lowest intensity in the wing veins (Figure 3E). In contrast to the other three IRM proteins, SNS can only be detected at the membranes of SOPs (Figure 3H) and is a good marker to follow their development.

As in other tissues, IRM proteins have a strong impact on each other's localization during wing development. As an example, we show the effect of global misexpression of *hbs* via *Mz*1369-Gal4 on kirre and SNS localization (Figure 8F). SNS is no longer found only in the apical contact zone. Much SNS is found in vesicular bodies instead. Further, kirre no longer highlights the contact sites of epidermal cells to the SOPs. It also seems to be inhomoneously distributed along the contacts of epidermal cells in the narrow neurogenic region and seems to accumulate in vesicular bodies as well (arrow in Figure 8F).

A wild-type adult wing margin is shown in Figure 8B. The anterior wing margin consists of three rows of bristles. The dorsal and ventral sides bear regular-spaced chemosensory recurved bristles. Quantitative analysis of the ventral triple row bristles shows that their spacing ranges from 3 to 5 bristles. Over 90% of the bristles show 3 or 4 intervening mechanosensory bristles (Figure 8A). Interference with IRM protein expression by various methods (e.g., RNAi, misexpression, or mutant analysis) invariably leads to a diverse range of mutant phenotypes in the anterior wing margin, ranging from light disruptions of the spacing pattern, as in $irreC^{UB883}$ (Figure 8A), to the complete disruption of a regular pattern by misexpression of *irreC*/*rst* in the SOPs via *neuralized*-GAL4 (Figure 8A and 8D). In addition, the number of

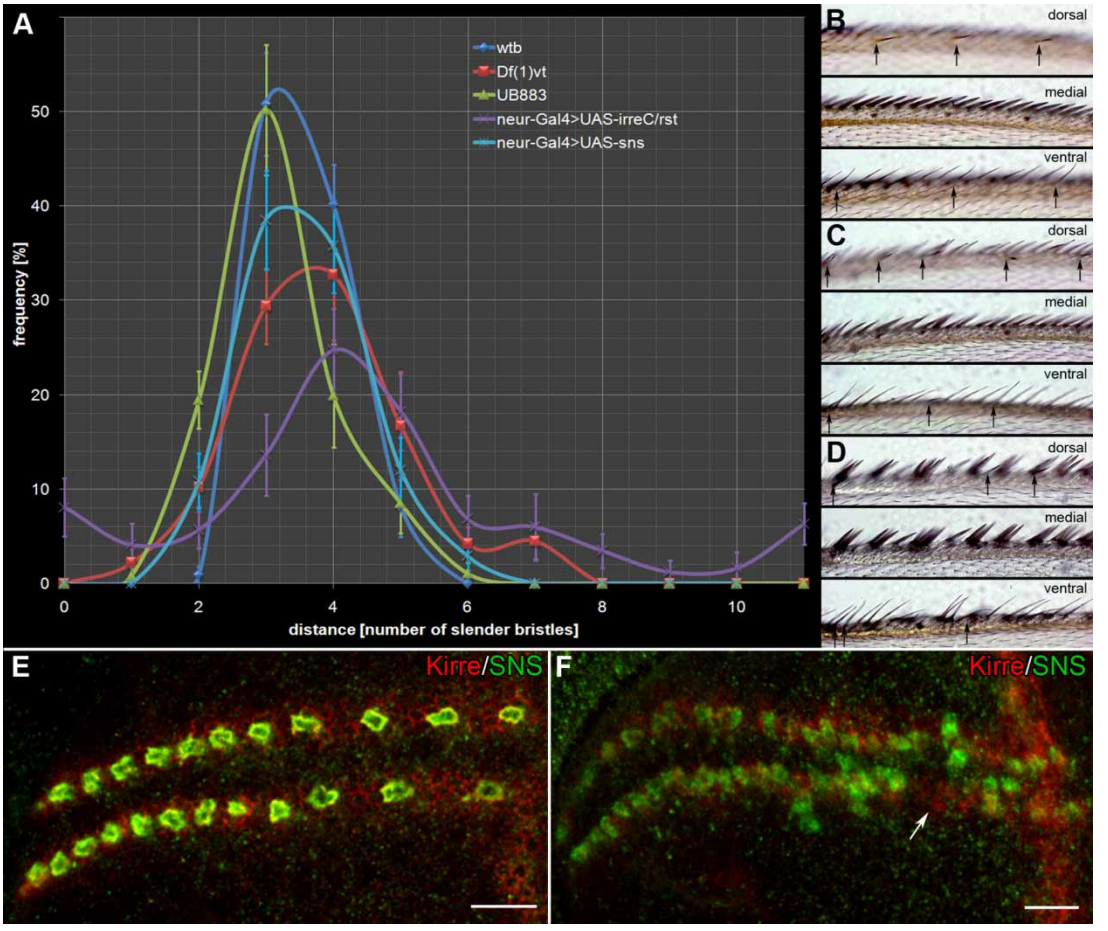

Figure 8. Irre cell recognition module (IRM) proteins pattern the array of sensory bristles at the anterior wing margin. (**A**) The relative distance between recurved bristles is measured by the number of intervening slender bristles. The frequency of the occurrence of a given number of intervening slender bristles is plotted against this number. In the wild-type control (wtb, dark blue curve), over 90% of recurved bristles at the ventral row show a spacing of three to four intervening slender bristles. The distribution in *irreC*^{UB883} (green curve) is somewhat shifted to smaller distances, but the pattern is still highly regular. In *Df(1)vt* (red curve), distances are irregular. Spacing ranges from one to seven intervening slender bristles. Misexpression of *irreC/rst* in the sensory precursors (SOPs) lead to an extreme phenotype (magenta curve), where spacing ranges from 0 to over 10. This is in contrast to the overexpression of *sns* in SOPs, which shows a rather mild phenotype (light blue curve). For all genotypes, $N = 10$. Error bars denote the standard error of the mean. (**B**–**D**) Photographs of different genotypes at three different focal planes. Arrows point to the recurved bristles. (**B**) The anterior wing margin of wtb. (**C**) Anterior wing margin of *Df(1)vt*. The disruption of the pattern is visible on the dorsal and ventral side of the margin. (**D**) Misexpression of *irreC/rst* via *neuralized-Gal4* in the SOPs leads to a strong disruption of the spacing pattern at the wing margin. No regular spacing pattern of recurved bristles is visible anymore, and additionally, the row of stout bristles in the medial triple row is disrupted. (**E**–**F**) Projection view of confocal images showing the neurogenic region of the wing margin in L3. (**E**) The wild-type control shows a regular spaced pattern already at this stage, with the largest intervals between the SOPs [marked by sticks and stones (SNS) immunoreactivity] at the presumptive tip of the wing. (**F**) Global misexpression of *UAS-hbs* with the driver line, *Mz1369-Gal4*, leads to a disruption of the pattern of SOPs and also to a relocalization of kirre and SNS immunoreactivity. Both proteins are no longer specifically accumulated at the contact sites of SOPs with surrounding cells. Kirre immunoreactivity is shown in red, SNS immunoreactivity in green. Antibodies used: antikirre (A126i; Kreisköther et al., 2006), anti-IrreC/Rst (Mab24A5.1; Schneider et al., 1995), anti-SNS (Kesper et al., 2007), and anti-Hbs (AS14). Scale bars, 10 μm.

recurved bristles is reduced in this genotype. The deficiency, *Df(1)vt*, which affects the *irreC/rst* and *kirre* genes, shows a much stronger phenotype than the *P*-element insertion allele, *irreC*^{UB883}. In this respect, the anterior wing margin phenocopies the effects seen in muscle fusion, where the most severe phenotypes are obtained when both proteins are affected (Strünkelnberg et al., 2001). In general, IRM proteins have a strong impact on the spacing pattern if they are absent or when they are misexpressed in the wrong cell type. This point becomes visible when the effects of misexpressing *sns* via *neuralized-Gal4* are compared to the misexpression of

irreC/rst with this driver line. The SOPs that normally express *sns* are insensitive against its overexpression, while the misexpression of *irreC/rst* results in the loss of bristles.

In summary, IRM proteins are required for the regular spacing of sensory organs in imaginal discs. The distribution of the four proteins on the participating cell types differs somewhat from the pattern observed in muscle fusion and IPC sorting. SNS seems to be located in sensory precursors, while Hbs, IrreC/Rst, and kirre are located on the surrounding cells of the neurogenic region. This difference in IRM distribution might be helpful for keeping sensory precursors more than one cell layer apart.

Regularly spaced patterns of sensory organs are frequently observed in nature, not only in *Drosophila*. Bristles of other arthropods or stereocilia of hair cells in the inner ear of vertebrates are good examples (Renaud & Simpson, 2001; Lewis & Davies, 2002). The mouse ortholog of kirre, mkirre, is present in the inner ear at E17.5 (Ueno et al., 2003). It would be challenging to investigate the role of mouse IRM proteins more closely in this context.

IRM PROTEINS IN NEURAL DEVELOPMENT

Wiring a three-dimensional (3D) brain requires that dendritic and axonal terminals of different neurons, as well as glial processes, contact each other in a highly nonrandom fashion. This is doubtlessly a far more formidable task than arranging cells in a 2D epithelial field. Nevertheless, some of the molecular machinery working in epithelia may well be employed in the brain as well.

Mutational analysis, gene knockdown, and overexpression studies of IrreC/Rst and other IRM members have shown that their tightly regulated expression pattern is already required during stages of axonal pathfinding (Boschert et al., 1990; Schneider et al., 1995; Chaudhary et al., in preparation). However, the expression in the optic neuropil of all these proteins persists into the stages of target selection and synaptogenesis (Figure 3I–3L). It is this aspect of IRM function—after axonal pathfinding has been completed—on which we focus here.

We put forward here the working hypothesis that during target recognition, the IRM proteins are involved in the sorting of dendritic and axonal arborizations in the neuropil layers of the optic lobe. As a prerequisite for such an analysis, we present data showing that IrreC/Rst and kirre are expressed in overlapping sets of columnar neurons.

Identification of cell types underlying the expression pattern shown in Figure 3 is problematic from an inspection of protein localization alone. The *irreC/rst* and *kirre* genes are located head to head at the tip of the X-chromosome (3C5-6) separated by 128 kb, so they could, in principle, share common regulatory elements. *kirre* is located only 2 kb upstream of the *Notch* transcription unit, and so far, only a regulatory region of 12 kb 5′ of *irreC/rst* has been dissected, containing overlapping modules for mesoderm and optic-lobe expression (Apitz et al., 2004, 2005). We tested several GAL4 insertions within the boundaries of the regulatory region of the *irreC/rst* and *kirre* genes for the match of green flourescent protein (GFP) reporter gene expression to the immunoreactivity pattern of the two corresponding proteins. It turned out that the pattern of *UAS-mCD8::GFP* expression produced by the GAL4 insertion NP2044 36 bp upstream of the *irreC/rst* gene matches closely the IrreC/Rst immunoreactivity (Figure 9A–9C). MARCM studies (Lee & Luo, 2001), using the strain NP2044, showed a large assembly of columnar neurons, examples of which are shown in Figure 9 (background immunoreactivity is anti-IrreC/Rst). Lamina monopolar neurons L1, L3, and L4 were frequently encountered (Figure 9F) as well as the transmedulla neurons, TM1, TM2, TM3, and TM4 (Figure 9G–9J). Although layer M10 is not strongly IrreC/Rst positive, T4 neurons were often seen, suggesting that IrreC/Rst is not present in their medullar dendrites. Quite remarkable is the contribution of the large set of local interneurons of the proximal medulla (PM-neurons; Fischbach & Dittrich, 1989) to the strongly columnar, doughnut-like labeling of medulla layer M9 (Figure 9E; see also Hiesinger et al., 1999, their Figure 2C). The GFP-ositive cell bodies of the PMs can be seen as dorsal and ventral clusters in Figure 9A and 9C. Noteworthy are also LC12 neurons (Otsuna & Ito, 2006) that connect the lobula to a single optic glomerulus that is strongly IrreC/Rst immunoreactive. The cluster of LC12 cell bodies is strongly GFP positive (Figure 9A and 9C). Figure 9D depicts one of these cells singled out by MARCM. It can clearly be seen that the arborizations of LC12 cells extend throughout the optic glomerulus, but that the arborizations in the lobula are columnar. Therefore, visuotopy is lost at the level of the optic glomeruli. The set of neuronal cell types found to be positive in the strain NP2044 is summarized in Figure 9K.

We also performed MARCM studies using the Gal4 insertion NP2273 844bp 5′ of the *kirre* gene and were able to identify several columnar cell types (Figure 10; background immunoreactivity is anti-Kirre). Most instructive are the labelling patterns of lamina monopolar neurons L1, L3, and L4 (Figure 10H–10P). Kirre immunoreactivity in the lamina neuropil is restricted to the proximal layer, where the collaterals of the L4 neurons reside. These collaterals are known to be partially presynaptic (Meinertzhagen & O'Neil, 1991). In contrast to their terminals in the medulla, the dendrites of L1 and L3 in the lamina are obviously kirre negative. The set of

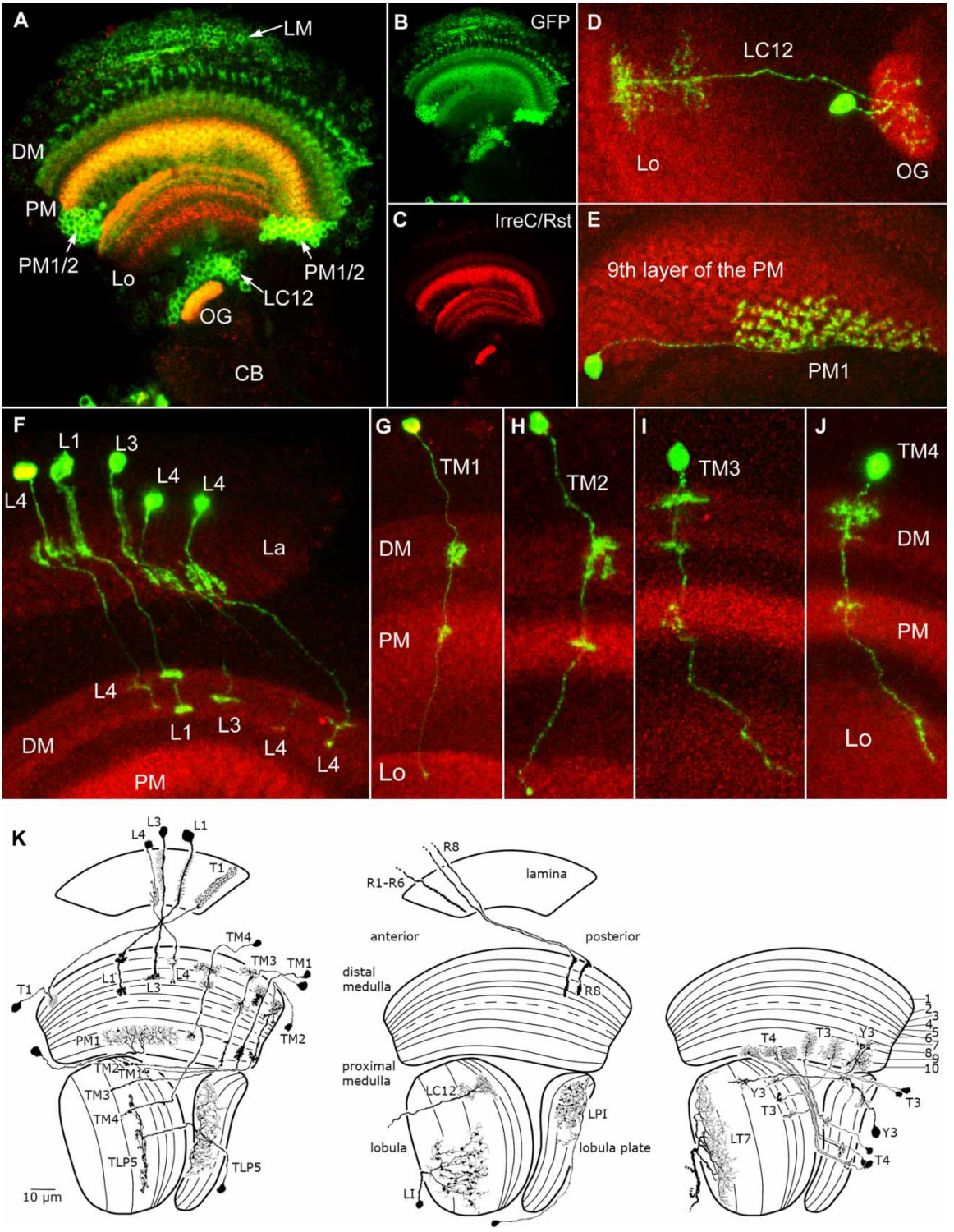

Figure 9. Examples of MARCM results using the GAL4-insertion of NP2044 upstream of *irreC/rst*. (**A**–**C**) *Gal4*^{NP2044} expression in the optic lobe visualized by mCD8::GFP. Arrows point to the prominent cell bodies of lamina monopolar cells (LM), PM1 and PM2 cells (PM 1/2), and LC12 cells (LC12). (**D**–**J**) Projection views of confocal stacks of different neurons. (**D**) Lobula columnar cell LC12. The optic glomerulus, consisting of the presynaptic termini of LC12 cells, is strongly irregular chiasm C/roughest (IrreC/Rst) positive. (**E**) Amacrine cell PM1 arborizing in layer M9. This layer is strongly GFP (**B**) and IrreC/Rst (**C**) positive. (**F**) Lamina monopolar cells L1, L3, and L4. (**G**) Transmedulla cell TM1. (**H**) Transmedulla cell TM2. (**I**) Transmedulla cell TM3. (**J**) Transmedulla cell TM4. (**K**) Comparison of all the neurons identified in the screen of NP2044 to their Golgi drawings (modified after Fischbach & Dittrich, 1989). Red: anti-IrreC/Rst (Mab24A5.1); green: anti-mCD8. La, lamina; DM, distal medulla; PM, proximal medulla; Lo, lobula; OG, optic glomerulus; CB, central brain.

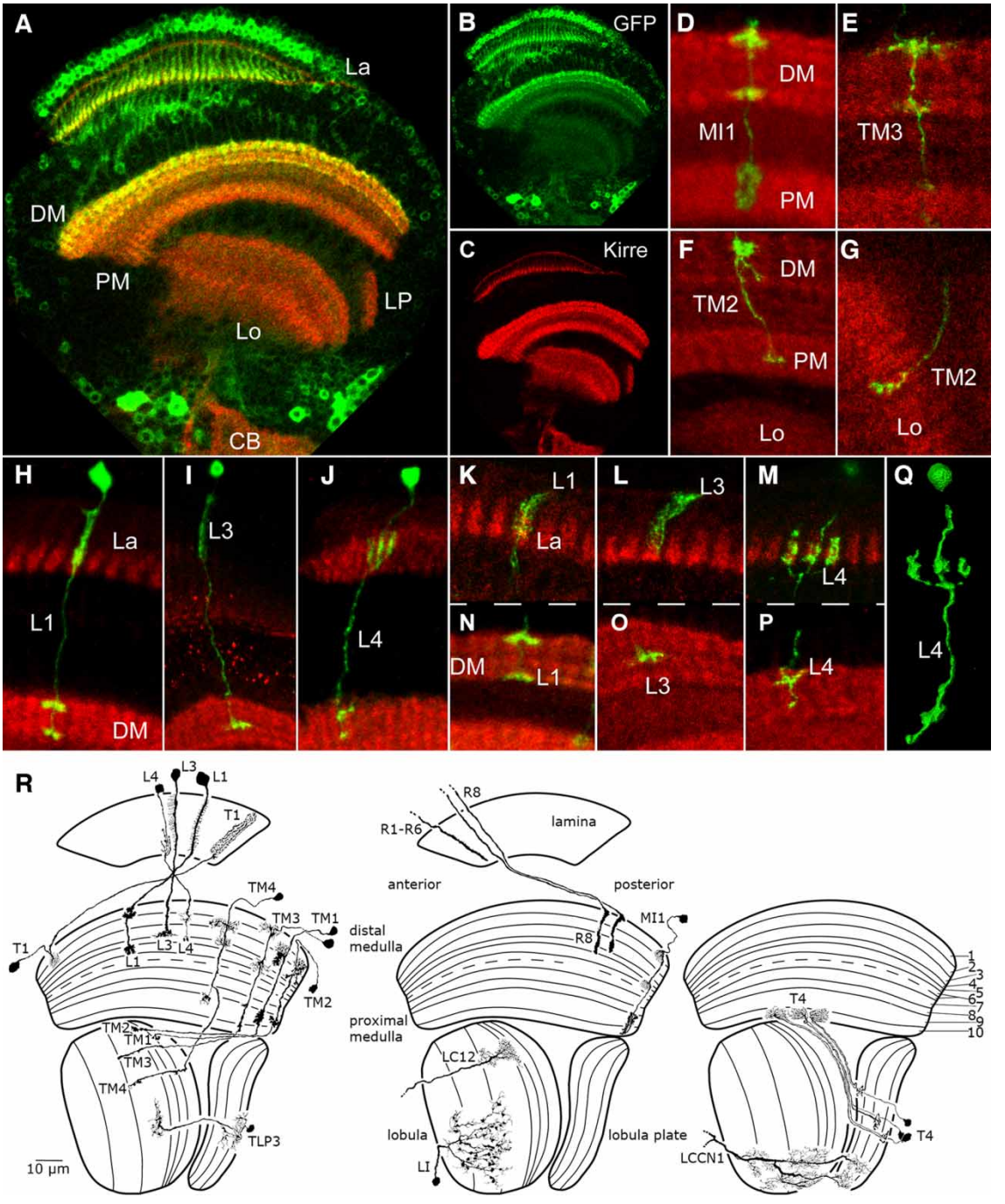

Figure 10. Examples of MARCM results using the GAL4-insertion NP2273 upstream of *kirre*. (**A**–**C**) *Gal4*^{NP2273} expression in the optic lobe visualized by mCD8::GFP. The prominent groups of cell bodies visible for NP2044 are not present in this line. (**D**–**P**) Projection views of confocal stacks of different neurons. Where detailed views of selected parts of a cell are shown, only the necessary focal planes have been used for merging the Z-stack. Thus, the antikirre background staining is more defined in these cases. (**D**) Arborization of the medulla intrinsic cell MI1. (**E**) Arborization of the transmedulla cell TM3. (**F**) Arborizations of the transmedulla cell TM2 in the medulla. (**G**) Terminus of a TM2 cell in the lobula. (**H**) Lamina monopolar cell L1. (**I**) Lamina monopolar cell L3. (**J**) Lamina monopolar cell L4. (**K**–**M**) The lamina arborizations of the L1 and L3 neurons do not colocalize with the proximal antikirre-positive lamina layer; the collaterals of the L4 cells, however, fit perfectly (**M**). The medulla terminals of the lamina monopolar neurons arborize in the kirre immunoreactive layers of the distal medulla (**N**–**P**). (**Q**) *IsoSurface* three-dimensional reconstruction of an L4 cell. (**R**) Comparison of all the neurons identified in the screen of NP2273 to their Golgi drawings (modified after Fischbach & Dittrich, 1989). Red: antikirre (A126i); green: anti-mCD8. La, lamina; DM, distal medulla; PM, proximal medulla; Lo, lobula; LP, lobula plate; CB, central brain.

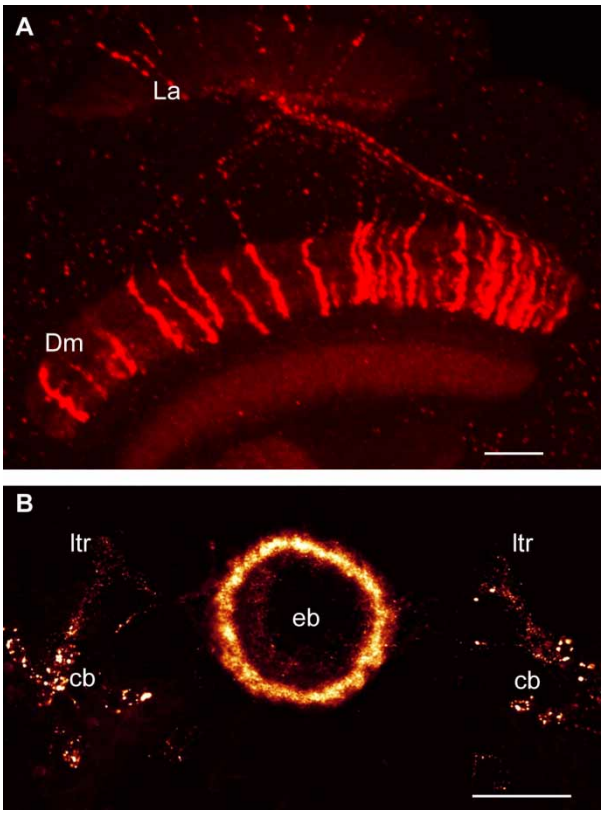

Figure 11. Selective transport of irregular chiasm C/roughest (IrreC/Rst) to presynaptic terminals. (**A**) Overexpressing IrreC/Rst in R7 neurons in *panR7-Gal4;UAS-irreC/rst* pupae results in its specific transport to the presynaptic terminals in the distal medulla neuropil. Please note that all R7-cell axons project through the first optic chiasm and display punctuated IrreC/Rst immunoreactivity contained in vesicular bodies. However, in the presynaptic terminals inside the distal medulla, IrreC/Rst immunoreactivity is found at the membranes. The spiny shapes, arrangement, and irregular projection depths of the terminals are a consequence of IrreC/Rst overexpression. Antibody used: Mab24A5.1 at stage 55% of pupal development. La, lamina; Dm, distal medulla; Pm, proximal medulla; lo, lobula; Lp, lobula plate. Scale bar, 25 μm. (**B**) Misexpression of IrreC/Rst in the population of the outer ring neurons of the ellipsoid body (eb) in *Gal4^{124};UAS-irreC/rst* pupae. The protein accumulates in the presynaptic terminals aranged in a ring inside the ellipsoid body. In the other cellular compartments, only vesicular immunoreactivity can be observed. cb, cell bodies; eb, ellipsoid body; ltr, lateral.

neuronal cell types found to be positive in the strain NP2273 is summarized in 10R.

It is apparent from the data of Figures 9 and 10 that kirre and IrreC/Rst are not transported to all neuropil compartments of interneurons. The PM local interneurons may be an exception, but they could well have distributed pre- and postsynaptic sites all over their arborizations. In projection neurons, there seems to be a preferential transport to presynaptic sites. This can be recognized in Figure 9D (LC12 cells have presynaptic termini at the optic glomerulus; Otsuna & Ito, 2006), in Figure 10G (strong kirre immunoreactivity at the termini of TM2 cells), 10M (presynaptic collaterals of L4 cells are kirre positive), and 10N–10P (layers of kirre immunoreactivity overlap with the termini of lamina monopolar cells). In addition, when IrreC/Rst proteins are overexpressed in retinula cells, preferential transport of the protein to the presynaptic terminals can be observed (Figure 11A). This selective transport to the axonal terminals of retinula cells is also observed for kirre, but it does not take place with mis- or overexpressed SNS and Hbs.

When misexpressed in central brain neurons with a clear spatial separation of dendritic input and axonal output regions, SNS and IrreC/Rst are selectively transported into the dendritic and axonal parts, respectively: The GAL4 line, OK107, drives the expression of UAS transgenes in Kenyon cells of the MBs (Connolly et al., 1996). Misexpressed SNS is exclusively transported to the dendrites in the calyx region, while misexpressed IrreC/Rst is found in the lobes. Similarly, the GAL4 line, c507, drives expression in the ring neurons of the ellipsoid body (Renn et al., 1999). Misexpressed IrreC/Rst localizes in the synaptobrevin positive axonal terminals, whereas misexpressed SNS accumulates in the arborizations of the lateral triangles, which are known to contain the dendrites of the input neurons of the ellipsoid body in the locust (Träger et al., 2008). The specific localization of misexpressed IrreC/Rst in the axonal terminals of the outer ring neurons of the ellipsoid body was also reported by Reiter et al. (2000), using the GAL4 line, KL124 (Figure 11B).

Taking into account the data presented, it seems likely that the IRM genes are not only expressed in different, possibly overlapping, cell-type populations of the optic lobe, but that the proteins are differentially located on dendritic and axonal arborizations in the neuropil layers. Preliminary results indicate that connectivity of cells can be altered when IRM protein levels are manipulated in defined cell types.

OUTLOOK

Now that it has become clear that IRM proteins in *Drosophila* are involved in the recognition between different cell types and are required for the correct sorting of cells in epithelia, the focus of future research should be on their role in neural development. A first step has to be the identification of the cell types involved and the examination of the preferential distribution of the proteins to dendritic and axonal compartments. The analysis of their role in optic-lobe development can, then, be based on the knowledge already accumulated about the

development, structure, and function of the optic lobes of *Drosophila* (reviewed in Fischbach & Hiesinger, 2008; Ting & Lee, 2007; Mast et al., 2006; Meinertzhagen & Hanson, 1993). Until recently, few specific markers and probes were available for visual interneurons. Accordingly, only a few papers explicitly dealt with the development, structure, and function of visual interneurons in *Drosophila* (Meinertzhagen et al., 2000; Otsuna & Ito, 2006; Rister et al., 2007; Millard et al., 2007; Raghu et al., 2007; Joesch et al., 2008). Due to their large number and small size, the interneurons of the medulla were especially neglected. In addition, not much was known about the connectivity of the medullar terminals of the lamina monopolar cells. Only recently, these unknown circuits of the medulla are being made accessible for genetic (Morante & Desplan, 2008), as well as ultrastructural, analysis (Takemura et al., 2008). Knowledge about neuronal connectivity in the medulla and cell-type-specific tools will greatly promote the investigation of IRM protein function in this neuropil. In *C. elegans*, a function of IRM proteins in the localization and stabilization of presynaptic sites has been reported (Shen & Bargmann, 2003; Shen et al., 2004). The development of stereotyped synapses of the HSNL motor neuron was investigated *in vivo*. The SYG-1 protein (Table 1) is localized along the HSNL motor axon at the site of persisting synapses by heterophilic interactions with SYG-2 (Table 1) in the guidepost epithelial cells and inhibits synapse degradation by inhibiting the assembly of an E3 ubiquitin ligase complex (Ding et al., 2007). A similar role in other species has yet to be shown.

Although it was found that proteins of the kirre/NEPH- and SNS/nephrin subfamilies are expressed in neighboring cell types in the nervous system of vertebrates (e.g., Beltcheva et al., 2003; Tamura et al., 2005; Gerke et al., 2006; Morikawa et al., 2007), there is only cursory information as to their function thus far. The continuing experimental work and accumulation of new knowledge on the IRM members and their role in invertebrates will undoubtedly be helpful in guiding the research in vertebrate species as well.

ACKNOWLEDGMENTS

The authors thank Margit Böhler and Weronika Brinkmann for their expert technical assistance. Mary Baylies and Susan Abmayr provided batches of their antibodies against Hbs and SNS that were of great help until substituted by our own. The authors also thank Kei Ito and the NP consortium for providing NP-lines. This work was supported by SFB 505 and the Deutsche Forschungsgemeinschaft. Drs. Sujin Bao, Randy Cassada, Gert H. de Couet, Martin Höhne, and Tobias Huber read the manuscript and gave valuable advice.

REFERENCES

Apitz, H., Kambacheld, M., Straube, A., Höhne, M., Ramos, G. P. R., & Fischbach, K. F. (2004). Identification of regulatory modules mediating specific expression of the *roughest* gene in *Drosophila melanogaster*. *Dev Genes Evol, 214*, 453–459.

Apitz, H., Strünkelnberg, M., de Couet, H. G., & Fischbach, K. F. (2005). Single-minded, Dmef2, Pointed, and Su(H) act on identified regulatory sequences of the *roughest* gene in *Drosophila melanogaster*. *Dev Genes Evol, 215*, 460–469.

Artero, R. D., Castanon, I., & Baylies, M. K. (2001). The immunoglobulin-like protein Hibris functions as a dose-dependent regulator of myoblast fusion and is differentially controlled by Ras and Notch signaling. *Development, 128*, 4251–4264.

Balagopalan, L., Chen, M. H., Geisbrecht, E. R., & Abmayr, S. M. (2006). The CDM superfamily protein MBC directs myoblast fusion through a mechanism that requires phosphatidylinositol 3,4,5-triphosphate binding but is independent of direct interaction with DCrk. *Mol Cell Biol, 26*, 9442–9455.

Bao, S., & Cagan, R. (2005). Preferential adhesion mediated by Hibris and Roughest regulates morphogenesis and patterning in the *Drosophila* eye. *Dev Cell, 8*, 925–935.

Bairoch, A. (1991). PROSITE: a dictionary of sites and patterns in proteins. *Nucleic Acids Res, 19 Suppl*, 2241–2245.

Bazigou, E., Apitz, H., Johansson, J., Loren, C. E., Hirst, E. M., Chen, P. L., et al. (2007). Anterograde Jelly belly and Alk receptor tyrosine kinase signaling mediates retinal axon targeting in *Drosophila*. *Cell, 128*, 961–975.

Beltcheva, O., Kontusaari, S., Fetissov, S., Putaala, H., Kilpelainen, P., Hokfelt, T., et al. (2003). Alternatively used promoters and distinct elements direct tissue-specific expression of nephrin. *J Am Soc Nephrol, 14*, 352–358.

Boschert, U., Ramos, R. G. P., Tix, S., Technau, G. M., & Fischbach, K. F. (1990). Genetic and developmental analysis of irreC, a genetic function required for optic chiasm formation in *Drosophila*. *J Neurogen, 6*, 153–171.

Bour, B. A., Chakravarti, M., West, J. M., & Abmayr, S. M. (2000). *Drosophila* SNS, a member of the immunoglobulin superfamily that is essential for myoblast fusion. *Genes Dev, 14*, 1498–1511.

Chen, E. H., & Olson, E. N. (2001). Antisocial, an intracellular adaptor protein, is required for myoblast fusion in *Drosophila*. *Dev Cell, 1*, 705–715.

Chen, E. H., & Olson, E. N. (2004). Towards a molecular pathway for myoblast fusion in *Drosophila*. *Trends Cell Biol, 14*, 452–460.

Clamp, M., Cuff, J., Searle, S. M., & Barton, G. J. (2004). The Jalview Java alignment editor. *Bioinformatics, 20*, 426–427

Connolly, J. B., Roberts, I. J., Armstrong, J. D., Kaiser, K., Forte, M., Tully, T., et al. (1996). Associative learning disrupted by impaired Gs signaling in *Drosophila* mushroom bodies. *Science, 274*, 2104–2107.

Delaney, S.J., Hayward, D. C., Barleben, F., Fischbach, K. F., & Gabor Miklos, G. L. (1991). Molecular cloning and analysis of small optic lobes, a structural brain gene of

Drosophila melanogaster. *Proc Natl Acad Sci USA, 88*, 7214–7218.

Ding, M., Chao, D., Wang, G., & Shen, K. (2007). Spatial regulation of an E3 ubiquitin ligase directs selective synapse elimination. *Science (New York)*, *317*, 947–951.

Doberstein, S. K., Fetter, R. D., Mehta, A. Y., & Goodman, C. S. (1997). Genetic analysis of myoblast fusion: blown fuse is required for progression beyond the prefusion complex. *J Cell Biol*, *136*, 1249–1261.

Dushay, M. S., Rosbash, M., & Hall, J. C. (1989). The disconnected visual system mutations in *Drosophila melanogaster* drastically disrupt circadian rhythms. *J Biol Rhythms, 4*, 1–27.

Dworak, H. A., Charles, M. A., Pellerano, L. B., & Sink, H. (2001). Characterization of *Drosophila hibris*, a gene related to human nephrin. *Development, 128*, 4265–4276

Fischbach, K. F., & Dittrich A. P. M. (1989). The optic lobe of *Drosophila melanogaster*. Part I, a Golgi analysis of wild-type structure. *Cell Tissue Res, 258*, 441–475.

Fischbach, K. F., & Heisenberg, M. (1981). Structural brain mutant of *Drosophila melanogaster* with reduced cell number in the medulla cortex and with normal optomotor yaw response. *Proc Natl Acad Sci USA, 78*, 1105–1109.

Fischbach, K. F., & Hiesinger, P. R. (2008). Optic lobe development in brain development in *Drosophila*. In: Technau, G., (Ed.). *Brain Development in* Drosophila melanogaster (pp 115–136). Landes Biosciences and Springer Science+Business Media.

Galletta, B. J., Chakravarti, M., Banerjee, R., & Abmayr, S. M. (2004). SNS, adhesive properties, localization requirements, and ectodomain dependence in S2 cells and embryonic myoblasts. *Mech Dev, 121*, 1455–1468.

Gerke, P., Benzing, T., Höhne, M., Kispert, A., Frotscher, M., Walz, G., et al. (2006). Neuronal expression and interaction with the synaptic protein CASK suggest a role for Neph1 and Neph2 in synaptogenesis. *J Comp Neurol, 498*, 466–475.

Gerke, P., Huber, T. B., Sellin, L., Benzing, T., & Walz, G. (2003). Homodimerization and heterodimerization of the glomerular podocyte proteins nephrin and NEPH1. *J Am Soc Nephrol, 14*, 918–926.

Gerke, P., Sellin, L., Kretz, O., Petraschka, D., Zentgraf, H., Benzing, T., et al. (2005). NEPH2 is located at the glomerular slit diaphragm, interacts with nephrin, and is cleaved from podocytes by metalloproteinases. *J Am Soc Nephrol, 16*, 1693–1702.

Gorski, S. M., Brachmann, C. B., Tanenbaum, S. B., & Cagan, R. L. (2000). Delta and notch promote correct localization of irreC-rst. *Cell Death Different*, *7*, 1011–1013.

Grzeschik, N. A., & Knust, E. (2005). IrreC/Rst-mediated cell sorting during *Drosophila* pupal eye development depends on proper localisation of DE-cadherin. *Development, 132*, 2035–2045.

Hanesch, U., Fischbach, K. F., & Heisenberg, M. (1989). Neuronal architecture of the central complex in *Drosophila melanogaster*. *Cell Tissue Res, 257*, 343–366.

Hartenstein, V., & Posakony, J. W. (1989). Development of adult sensilla on the wing and notum of *Drosophila melanogaster*. *Development*, *107*, 389–405.

Heisenberg, M., & Boehl, K. (1979). Isolation of anatomical brain mutants of *Drosophila* by histological means. *Z Naturforsch, 34*, 143–147.

Heisenberg, M., Borst, A., Wagner, S., & Byers, D. (1985). *Drosophila* mushroom body mutants are deficient in olfactory learning. *J Neurogen, 2*, 1–30.

Hiesinger, P. R., Reiter, C., Schau, H., & Fischbach, K. F. (1999). Neuropil pattern formation and regulation of cell adhesion molecules in *Drosophila* optic lobe development. *J Neurosci*, *19*, 7548–7556.

Hofmann, K., & Stoffel, W. (1993). TMbase—a database of membrane-spanning proteins segments. *Biol Chem Hoppe-Seyler, 374*, 166.

Huber, T. B., & Benzing, T. (2005). The slit diaphragm, a signaling platform to regulate podocyte function. *Curr Opin Nephrol Hypertens, 14*, 211–216.

Huber, T. B., Hartleben, B., Kim, J., Schmidts, M., Schermer, B., Keil, A., et al. (2003a). Nephrin and CD2AP associate with phosphoinositide 3-OH kinase and stimulate AKT-dependent signaling. *Mol Cell Biol, 23*, 4917–4928.

Huber, T. B., Schmidts, M., Gerke, P., Schermer, B., Zahn, A., Hartleben, B., et al. (2003b). The carboxyl terminus of NEPH family members binds to the PDZ domain protein zonula occludens-1. *J Biol Chem, 278*, 13417–13421.

Joesch, M., Plett, J., Borst, A., & Reiff, D. F. (2008). Response properties of motion-sensitive visual interneurons in the lobula plate of *Drosophila melanogaster*. *Curr Biol, 18*, 368–374.

Kestilä, M., Lenkkeri, U., Männikkö, M., Lamerdin, J., McCready, P., Putaala, H., et al. (1998). Positionally cloned gene for a novel glomerular protein—nephrin—is mutated in congenital nephrotic syndrome. *Mol Cell, 1*, 575–582.

Kesper, D. A., Stute, C., Buttgereit, D., Kreiskother, N., Vishnu, S., Fischbach, K. F., et al. (2007). Myoblast fusion in *Drosophila melanogaster* is mediated through a fusion-restricted myogenic-adhesive structure (FuRMAS). *Dev Dyn, 236*, 404–415.

Kim, S., Shilagardi, K., Zhang, S., Hong, S., Sens, K., Bo, J., et al. (2007). A critical function for the actin cytoskeleton in targeted exocytosis of prefusion vesicles during myoblast fusion. *Dev Cell, 12*, 571–586.

Kocherlakota, K. S., Wu, J., McDermott, J., & Abmayr, S. M. (2008). Analysis of the cell adhesion molecule sticks-and-stones reveals multiple redundant functional domains, protein-interaction motifs and phosphorylated tyrosines that direct myoblast fusion in *Drosophila melanogaster*. *Genetics*, *178*, 1371–1383.

Kreisköther, N., Reichert, N., Buttgereit, D., Hertenstein, A., Fischbach, K. F., & Renkawitz-Pohl, R. (2006). *Drosophila* Rolling pebbles colocalises and putatively interacts with alpha-Actinin and the Sls isoform Zormin in the Z-discs of the sarcomere and with Dumbfounded/Kirre, alpha-Actinin, and Zormin in the terminal Z-discs. *J Muscle Res Cell Motil*, *27*, 93–106.

Laissue, P. P., Reiter, C., Hiesinger, P. R., Halter, S., Fischbach, K. F., & Stocker, R. F. (1999). Three-dimensional reconstruction of the antennal lobe in *Drosophila melanogaster*. *J Comp Neurol, 405*, 543–552.

Lee, T., & Luo, L. (2001). Mosaic analysis with a repressible cell marker (MARCM) for *Drosophila* neural development. *Trends Neurosci, 24*, 251–254.

Lewis, J., & Davies, A. (2002). Planar cell polarity in the inner ear: how do hair cells acquire their oriented structure? *J Neurobiol*, *53*, 190–201.

Liu, G., Kaw, B., Kurfis, J., Rahmanuddin, S., Kanwar, Y. S., & Chugh, S. S. (2003). Neph1 and Nephrin interaction in the slit diaphragm is an important determinant of glomerular permeability. *J Clin Invest, 112*, 209–221.

Liu, X. L., Kilpeläinen, P., Hellman, U., Sun, Y., Wartiovaara, J., Morgunova, E., et al. (2005). Characterization of the interactions of the nephrin intracellular domain. *FEBS J*, *272*, 228–243.

Massarwa, R., Carmon, S., Shilo, B. Z., & Schejter, E. D. (2007). WIP/WASp-based actin-polymerization machinery is essential for myoblast fusion in *Drosophila*. *Dev Cell, 12*, 557–569.

Mast, J. D., Prakash, S., Chen, P. L., & Clandinin, T. R. (2006). The mechanisms and molecules that connect photoreceptor axons to their targets in *Drosophila*. *Semin Cell Dev Biol, 17*, 42–49.

Meinertzhagen, I. A., & Hanson, T. E. (1993). The development of the optic lobe. In: Bate, M., Martinez-Arias, A. (Eds.). *The Development of* Drosophila melanogaster II. (pp 1363–1491). Cold Spring Harbor Press.

Meinertzhagen, I. A., & O'Neil, S. D. (1991). Synaptic organization of columnar elements in the lamina of the wild type in *Drosophila melanogaster*. *J Comp Neurol, 305*, 232–263.

Meinertzhagen, I. A., Piper, S. T., Sun, X. J., & Frohlich, A. (2000). Neurite morphogenesis of identified visual interneurons and its relationship to photoreceptor synaptogenesis in the flies, *Musca domestica* and *Drosophila melanogaster*. *Eur J Neurosci, 12*, 1342–1356.

Menon, S. D., & Chia, W. (2007). Actin on multiple fronts to generate a muscle fiber. *Dev Cell, 12*, 479–481.

Menon, S. D., Osman, Z., Chenchill, K., & Chia, W. (2005). A positive feedback loop between Dumbfounded and Rolling pebbles leads to myotube enlargement in *Drosophila*. *J Cell Biol*, *169*, 909–920.

Millard, S. S., Flanagan, J. J., Pappu, K. S., Wu, W., & Zipursky, S. L. (2007). Dscam2 mediates axonal tiling in the *Drosophila* visual system. *Nature, 447*, 720–724.

Morante, J., & Desplan, C. (2008). The color-vision pathway in the medulla of *Drosophila*. *Curr Biol, 18*, 553–564.

Morikawa, Y., Komori, T., Hisaoka, T., Ueno, H., Kitamura, T., & Senba, E. (2007). Expression of mKirre in the developing sensory pathways: its close apposition to nephrin-expressing cells. *Neuroscience, 150*, 880–886.

Mundel, P., Heid, H. W., Mundel, T. M., Krüger, M., Reiser, J., & Kriz, W. (1997). Synaptopodin: an actin-associated protein in telencephalic dendrites and renal podocytes. *J Cell Biol, 139*, 193–204.

Nolan, K. M., Barrett, K., Lu, Y., Hu, K. Q., Vincent, S., & Settleman, J. (1998). Myoblast city, the *Drosophila* homolog of DOCK180/CED-5, is required in a Rac-signaling pathway utilized for multiple developmental processes. *Genes Dev*, *12*, 3337–3342.

Otsuna, H., & Ito, K. (2006). Systematic analysis of the visual projection neurons of *Drosophila melanogaster*. I. lobula-specific pathways. *J Comp Neurol, 497*, 928–958.

Patel, M. R., Lehrman, E. K., Poon, V. Y., Grump, J. G., Zhen, M., Bargmann, C. I., et al. (2006). Hierarchical assembly of presynaptic components in defined *C. elegans* synapses. *Nat Neurosci, 9*, 1488–1498.

Pütz, M., Kesper, D. A., Buttgereit, D., & Renkawitz-Pohl, R. (2005). In *Drosophila melanogaster*, the Rolling pebbles isoform 6 (Rols6) is essential for proper Malpighian tubule morphology. *Mech Dev*, *122*, 1206–1217.

Raghu, S. V., Joesch, M., Borst, A., & Reiff, D. F. (2007). Synaptic organization of lobula plate tangential cells in *Drosophila*: gamma-aminobutyric acid receptors and chemical release sites. *J Comp Neurol, 502*, 598–610.

Ramos, R. G. P., Igloi, G. L., Lichte, B., Baumann, U., Maier, D., Schneider, T., et al. (1993). The irregular chiasm C-roughest locus of *Drosophila*, which affects axonal projections and programmed cell death, encodes a novel immunoglobulin-like protein. *Genes Dev, 7,* 2533–2547.

Rau, A., Buttgereit, D., Holz, A., Fetter, R., Doberstein, S. K., Paululat, A., et al. (2001). *rolling pebbles (rols)* is required in *Drosophila* muscle precursors for recruitment of myoblasts for fusion. *Development, 128*, 5061–5073.

Reddy, G. V., Reiter, C., Shanbhag, S., Fischbach, K. F., & Rodrigues, V. (1999). Irregular chiasm C–roughest, a member of the immunoglobulin superfamily, affects sense-organ spacing on the *Drosophila* antenna by influencing the positioning of founder cells on the disc ectoderm. *Dev Genes Evol, 209*, 581–591.

Reiter, C., Nie, Z., & Fischbach, K. F. (2000). Flybrain.org (Accession no. AA00075).

Reiter, C., Schimansky, T., Nie, Z., & Fischbach, K. F. (1996). Reorganization of membrane contacts prior to apoptosis in the *Drosophila* retina. The role of the IrreC/Rst protein. *Development, 122*, 1931–1940.

Renaud, O., & Simpson, P. (2001). *scabrous* modifies epithelial cell adhesion and extends the range of lateral signalling during development of the spaced bristle pattern in *Drosophila*. *Dev Biol, 240*, 361–376.

Renn, S. C. P., Armstrong, J. D., Yang, M., Wang, Z., An, X., Kaiser, K., et al. (1999). Genetic analysis of the *Drosophila* ellipsoid body neuropil: organization and development of the central complex. *J Neurobiol, 41*, 189–207.

Rister, J., Pauls, D., Schnell, B., Ting, C. Y., Lee, C. H., Sinakevitch, I., et al. (2007). Dissection of the peripheral motion channel in the visual system of *Drosophila melanogaster*. *Neuron, 56*, 155–170.

Rose, B. D., & Post, T. W. (2001). *Clinical Physiology of Acid-Base and Electrolyte Disorders*. McGraw-Hill Professional.

Ruiz-Gomez, M., Coutts, N., Price, A., Taylor, M. V., & Bate, M. (2000). *Drosophila dumbfounded*, a myoblast attractant essential for fusion. *Cell, 102*, 189–198.

Schneider, T., Reiter, C., Eule, E., Bader, B., Lichte, B., Nie, Z., et al. (1995). Neural recognition in *Drosophila*, restricted expression of *irreC*/*rst* is required for normal axonal projections of columnar neurons. *Neuron, 15*, 259–271

Sellin, L., Huber, T. B., Gerke, P., Quack, I., Pavenstadt, H., & Walz, G. (2002). NEPH1 defines a novel family of podocin interacting proteins. *FASEB J, 17*, 115–117.

Serra-Pages, C., Medley, Q. G., Tang, M., Hart, A., & Streuli, M. (1998). Liprins, a family of LAR transmembrane protein-tyrosine phosphatase-interacting proteins. *J Biol Chem, 273*, 15611–15620.

Shen, K., & Bargmann, C. I. (2003). The immunoglobulin superfamily protein Syg-1 determines the location of specific synapses in *C. elegans*. *Cell, 112*, 619–630.

Shen, K., Fetter, R. D., & Bargmann, C. I. (2004). Synaptic specificity is generated by the synaptic guidepost protein SYG-2 and its receptor, Syg-1. *Cell, 116*, 869–881.

Srinivas, B. P., Woo, J., Leong, W. Y., & Roy, S. (2007). A conserved molecular pathway mediates myoblast fusion in insects and vertebrates. *Nat Genet, 39*, 781–786.

Steller, H., Fischbach, K. F., & Rubin, G. M. (1987). Disconnected: a locus required for neuronal pathway formation in the visual system of *Drosophila*. *Cell, 50*, 1139–1153.

Stocker, R. F., Lienhard, M. C., Borst, A., & Fischbach, K. F. (1990). Neuronal architecture of the antennal lobe in *Drosophila melanogaster*. *Cell Tissue Res, 262*, 9–34.

Strünkelnberg, M., Bonengel, B., Moda, L. M., Hertenstein, A., de Couet, H. G., Ramos, R. G. P., et al. (2001). *rst* and its paralogue *kirre* act redundantly during embryonic muscle development in *Drosophila*. *Development, 128*, 4229–4239.

Takemura S. Y., Lu Z., & Meinertzhagen I. A. (2008). Synaptic circuits of the *Drosophila* optic lobe: the input terminals to the medulla. *J Comp Neurol, 509*, 493–513

Tamura, S., Morikawa, Y., Hisaoka, T., Ueno, H., Kitamura, T., & Senba, E. (2005). Expression of mKirre, a mammalian homolog of *Drosophila* kirre, in the developing and adult mouse brain. *Neuroscience, 133*, 615–624.

Ting, C. Y., & Lee, C. H. (2007). Visual circuit development in *Drosophila*. *Curr Opin Neurobiol, 17*, 65–72.

Thompson, J. D., Higgins, D. G., & Gibson, T. J. (1994). CLUSTAL W: improving the sensitivity of progressive multiple sequence alignment through sequence weighting, position-specific gap penalties, and weight matrix choice. *Nucleic Acids Res, 22*, 4673–4680.

Träger, U., Wagner, R., Bausenwein, B., & Homberg, U. (2008). A novel type of microglomerular synaptic complex in the polarization vision pathway of the locust brain. *J Comp Neurol*, *506*, 288–300.

Ueno, H., Sakita-Ishikawa, M., Morikawa, Y., Nakano, T., Kitamura, T., & Saito, M. (2003). A stromal cell–derived membrane protein that supports hematopoietic stem cells. *Nat Immunol*, *4*, 457–463.

Vishnu, S., Hertenstein, A., Betschinger, J., Knoblich, J. A., de Couet, H. G., & Fischbach, K. F. (2006). The adaptor protein X11Lα/Dmint1 interacts with the PDZ-binding domain of the cell recognition protein Rst in *Drosophila*. *Dev Biol, 289*, 296–307.

Wolff, T., & Ready, D. F. (1991). Cell death in normal and rough eye mutants of *Drosophila*. *Development, 113*, 825–839.